Linköping Studies in Science and Technology
Dissertation No. 1239

Protein Misfolding in Human Diseases

Karin Almstedt

Linköping University
INSTITUTE OF TECHNOLOGY

Biochemistry
Department of Physics, Chemistry and Biology
Linköping University, SE-581 83 Linköping, Sweden
Linköping 2009

The cover shows a Himalayan mountain range,
symbolizing a protein folding landscape.

During the course of the research underlying this thesis, Karin Almstedt was enrolled in Forum Scientium, a multidisciplinary doctoral program at Linköping University, Sweden.

Copyright © 2009 Karin Almstedt
ISBN: 978-91-7393-698-9
ISSN: 0345-7524
Printed in Sweden by LiU-Tryck
Linköping 2009

Never Stop Exploring

ABSTRACT

The studies in this thesis are focused on misfolded proteins involved in human disease.
There are several well known diseases that are due to aberrant protein folding. These types of diseases can be divided into three main categories:

1. Loss-of-function diseases
2. Gain-of-toxic-function diseases
3. Infectious misfolding diseases

Most *loss-of-function diseases* are caused by aberrant folding of important proteins. These proteins often misfold due to inherited mutations. The rare disease carbonic anhydrase II deficiency syndrome (CADS) can manifest in carriers of point mutations in the human carbonic anhydrase II (HCA II) gene. One mutation associated with CADS entails the His107Tyr (H107Y) substitution. We have demonstrated that the H107Y mutation is a remarkably destabilizing mutation influencing the folding behavior of HCA II. A mutational survey of position H107 and a neighboring conserved position E117 has been performed entailing the mutants H107A, H107F, H107N, E117A and the double mutants H107A/E117A and H107N/E117A. We have also shown that the binding of specific ligands can stabilize the disease causing mutant, and shift the folding equilibrium towards the native state, providing a starting point for small molecule drugs for CADS.

The only known infectious misfolding diseases are the prion diseases. The human prion diseases Kuru, Gerstmann-Sträussler-Scheinker disease (GSS) and variant Creutzfeldt-Jakob are characterized by depositions of amyloid plaque from misfolded prion protein (HuPrP) in various regions of the brain depending on disease. Amyloidogenesis of HuPrP is hence strongly correlated with prion disease. Amyloid fibrillation and oligomer formation of PrP in *in vitro* studies have so far been performed under conditions where mild to harsh conditions of denaturants of various sorts have been included. In this work we show the unusual behavior of recombinant human prion protein during protein aggregation and fibrillation when performed under non-denaturing conditions close to physiological. We show that HuPrP amyloid fibrils are spun and woven from disordered aggregates.

POPULÄRVETENSKAPLIG SAMMANFATTNING

I denna avhandling presenteras resultat från studier om hur proteiner som veckar sig på fel sätt kan orsaka sjukdom. Den bakomliggande orsaken till att proteiner veckar sig på fel sätt är ibland att olika mutationer i vår arvsmassa gör att en utav de aminosyror som bygger upp ett protein har blivit utbytt mot en annan aminosyra med andra egenskaper. När ett protein veckas fel och förlorar sin struktur förlorar det också sin funktion och på så sätt kan en viktig funktion i cellen sättas ur spel och orsaka sjukdom. Proteiner har mycket viktiga uppgifter i våra celler och hjälper oss t.ex. att ta upp syre, försvara oss mot bakterier och virus och att bryta ner slaggprodukter.

Studierna som presenteras här visar att när proteinet humant karboanhydras II, som finns i många olika vävnader i kroppen och är viktigt i många olika processer, muteras och blir instabilt, kollapsar ihop till en icke fungerande, halvveckad proteinklump. Det har undersökts hur det kan komma sig att bytet av en enda aminosyra (av 259 som finns i proteinet) kan orsaka den här stora förändringen. Det har visat sig att det inte är en aminosyras direkta kontakter med sina grannar som är den viktigaste parametern, utan snarare är det stora interaktionsnätverk som är viktiga när det gäller hur ett protein stabiliseras.

Det har även undersökts hur prionproteinet (som är det protein som bl. a. orsakar Creutzfeldt-Jakobs sjukdom) kan byta struktur från en korkskruvsliknande och funktionell form till en silkestrådsliknande form som klumpar ihop sig och kan bilda plack i hjärnan. Studierna visar att det först bildas bollar av ihopklumpade prionproteiner som sedan vävs ut till tunna fibrer.

INCLUDED PAPERS

This thesis is based on work presented in the following papers, which are listed below and included in the end of the thesis.

Paper I

Almstedt K., Lundqvist M., Carlsson J., Karlsson M., Persson B., Johnsson B-H., Carlsson U and Hammarström P. *Unfolding a folding disease: Folding, misfolding and aggregation of the marble brain syndrome-associated mutant H107Y of human carbonic anhydrase II.* (2004) J. Mol. Biol. **342**, 619-633.

Paper II

Almstedt K., Mårtensson L-G., Carlsson U. and Hammarström P. *Thermodynamic interrogation of a folding disease. Mutant mapping of position 107 in human carbonic anhydrase II linked to marble brain disease.* (2008) Biochemistry. **47**, 1288-1298.

Paper III

Almstedt K., Rafstedt T., Supuran C.T., Carlsson U. and Hammarström P. *Small-molecule suppression of misfolding of mutated human carbonic anhydrase II linked to marble brain disease.* In manuscript.

Paper IV

Almstedt K., Nyström S., Nilsson K. P. and Hammarström P. *Amyloid Fibrils of Human Prion Protein are Spun and Woven from Disordered Aggregates.*
In manuscript.

LIST OF ABBREVIATIONS

ALS	Amyotrophic lateral sclerosis
ANS	8-anilino-1-naphtalenesulfonic acid
BSE	Bovine spongiform encephalopathy
BTB	Bromthymol blue
CA	Carbonic anhydrase
CAA	Carbonic anhydrase activator
CADS	Carbonic anhydrase II deficiency syndrome
CAI	Carbonic anhydrase inhibitor
CD	Circular dichroism
CFTR	Cystic fibrosis transmembrane conductance regulator
CJD	Creutzfeldt-Jakob disease
DNA	Deoxyribonucleic acid
FFI	Fatal Familial Insomnia
GPI anchor	Glycosylphosphatidylinositol anchor
GSS	Gerstmann-Sträussler-Scheinker Syndrome
GuHCl	Guanidine hydrochloride
HCA II	Human carbonic anhydrase II (wild type)
HCA II$_{H107Y}$	HCA II$_{pwt}$ with a H107Y mutation
HCA II$_{pwt}$	Pseudo wild-type of HCA II with a C206S mutation
HuPrP$_{90-231}$	Human prion protein sequence 90-231
^{His}HuPrP$_{90-231}$	Human prion protein sequence 90-231 with an N-terminal hexa histidine tag
^{His}HuPrP$_{121-231}$	Human prion protein sequence 121-231 with an N-terminal hexa histidine tag
IAPP	Islet amyloid polypeptide
ICT	Internal charge transfer
NMR	Nuclear magnetic resonance

PRNP	Gene encoding the prion protein
PrP^C	Cellular form of prion protein
PrP^{Sc}	Disease associated scrapie form of prion protein
Q_0	Fraction of native contacts
R_g	Radius of gyration
RTA	Renal tubular acidosis
TEM	Transmission electron microscopy
ThT	Thioflavin T
TICT	Twisted internal charge transfer
TSE	Transmissible spongiform encephalopathy

TABLE OF CONTENTS

INTRODUCTION 5

PROTEIN STRUCTURE 9

- α-helix 10
- β-sheet 11

PROTEIN FOLDING AND MISFOLDING 12

- Protein folding models 13
- Protein aggregation 16
- Amyloid fibrils 17

THE MODEL PROTEINS 23

- Carbonic Anhydrase 23
  - Human carbonic anhydrase II 23
  - Inhibition and Activation of Carbonic Anhydrase 26
- Human Prion Protein 28

PROTEIN MISFOLDING DISEASES 33

- Carbonic Anhydrase II Deficiency Syndrome 35
- Transmissible Spongiform Encephalopathy 38
  - Sporadic CJD 39
  - Variant CJD 39
  - Inherited prion disease 41
  - Iatrogenic CJD 43

METHODS 45

- Site Directed Mutagenesis 45
- Enzyme Activity 45
- Fluorescence Spectroscopy 45
  - Fluorophores 47
- Circular Dichroism Spectroscopy 51
  - Far-UV CD Spectra 51
  - Near-UV CD Spectra 52
- Transmission Electron Microscopy 53
- Evaluation of protein stability 54
  - Stabilization by ligand binding 56

SUMMARY OF PAPERS 59

Paper I and II 59
The HCA $\mathrm{II}_{\mathrm{H107Y}}$ mutant has a native like active site 59
The native state of HCA $\mathrm{II}_{\mathrm{H107Y}}$ is extremely destabilized 60
HCA $\mathrm{II}_{\mathrm{H107Y}}$ unfolds via an intermediate that is not aggregation prone 62
Investigation of the H107 region in the HCA II structure 64
The destabilization of HCA $\mathrm{II}_{\mathrm{H107Y}}$ is due to long distance interactions 68
Paper III 70
Paper IV 76
Formation of amyloid fibrils of recombinant human PrP under physiological conditions 76
Amyloid fibrillation kinetics by Thioflavin T 77
Amyloid fibrils are formed after initial aggregation 78

CONCLUSIONS 81

ACKNOWLEDGEMENTS 85

REFERENCES 89

INTRODUCTION

Biochemistry has emerged as a dynamic science only within the past 100 years. Two major breakthroughs in the history of biochemistry are especially notable: i) The discovery of nucleic acids as information carrying molecules and ii) the roles of enzymes as catalysts. In 1897 Eduard Buchner showed that yeast extract could catalyze the fermentation of the sugar glucose to alcohol and carbon dioxide (Bornscheuer and Buchholz, 2005). Earlier it was believed that only living cells could catalyze such complex biological reactions. The last half of the 20th century saw tremendous advances in the area of structural biology, especially the structure of proteins. The first protein structures (myoglobin and haemoglobin) were solved in 1950s and 1960s by Kendrew and Perutz in Cambridge, UK. Since then many thousands of different protein structures have been determined and the understanding of protein chemistry has increased enormously. Proteins are involved in virtually every biological process in all living systems and their functions range from catalysis of chemical reactions to maintenance of the electrochemical potential across cell membranes. They are synthesized on ribosomes as linear chains of amino acids forming polypeptides in a specific order dictated from information encoded in the cellular DNA. In order to function it is important for the polypeptide chain to fold into the unique native three-dimensional structure that is characteristic for each protein. However, there appear to be only a limited number of folds, which indicates that different amino acid sequences can fold into almost identical structures.

There are many reasons why one should study protein folding and misfolding. A protein *in vivo* (in the biological environment in which it performs a certain task) has a specific conformation and if disrupted the functionality can be lost or it can even become toxic to the cell (Kelly, 2002; Sorgjerd et al., 2008). It is well known that proteins that are misfolded tend to form aggregates and/or interact improperly with the cell which can lead to cellular stress and cell death. Many diseases, such as Alzheimer's disease, cystic fibrosis, Creutzfeldt-Jakob disease and familial amyloidotic polyneuropathy, are known as misfolding diseases and/or amyloid diseases and are caused by misfolds of a protein, each specific for each disease, with incorrect conformation (Hammarstrom et al., 2002; Thomas et al., 1995).

One of the aims of my work has been to obtain a greater understanding of the effects point mutations can have on the stability and folding of a protein that is involved in human disease. The model used to achieve this is human carbonic anhydrase II, a protein which has been the focus of many previous studies regarding folding, stability and aggregation. This has been a great advantage to me in my studies, but the projects involving destabilized mutants have shown a variety of problems which have been stimulating to work with.

Another aim has been to try to elucidate the mechanism behind aggregation and amyloid fibril formation of the human prion protein, when working under native-like conditions. This is discussed in paper IV, which has been the most interesting study during my (so far) short research carrier and much still remains unresolved.

PROTEIN STRUCTURE

Proteins are long chains of amino acids linked together by peptide bonds with a positively charged amino group at one end and a negatively charged carboxyl group at the other end under neutral pH conditions. A sequence of different side chains runs along the chain. These differ for each of the different 20 amino acids that compose cellular proteins and the side chains have different properties, *i.e.* polar, hydrophobic or charged. The primary structure of a protein is the amino acid sequence, which determines the secondary, tertiary and quaternary structures.

When high resolution structures of proteins became available, it was noticed that the interior of the proteins were made up of hydrophobic side chains that formed a hydrophobic core inside the protein while the surface was composed of hydrophilic residues. To bring the side chains together into the core, the backbone of the protein must also fold into the interior. The backbone, however, is highly polar and hence hydrophilic, with both hydrogen bond donors (the NH group) and acceptors (the C=O group). This problem is solved by the formation of the secondary structure of a protein, when hydrogen bonds are formed within the interior of the protein. The secondary structure is usually of two types; α-helices or β-sheets.

a-helix

The right handed α-helix is the classic element of protein structure. This helix has 3.6 residues per turn with hydrogen bonds between the C=O of residue *n* and NH of residue *n+4*, see figure 1. All C=O and NH groups of a helix are joined by hydrogen bonds, except those at the ends, and therefore the ends of a helix are polar and are often found on the surface of the protein. The amino acid side chains project outward from the α-helix, and do not interfere with it (except for proline which is a α-helix breaker and is not found helices), although they are tilted slightly towards the amino end of the helix. Many α-helices are amphipathic, in that they have non-polar side chains along one side of the helical cylinder and polar side chains along the opposite side.

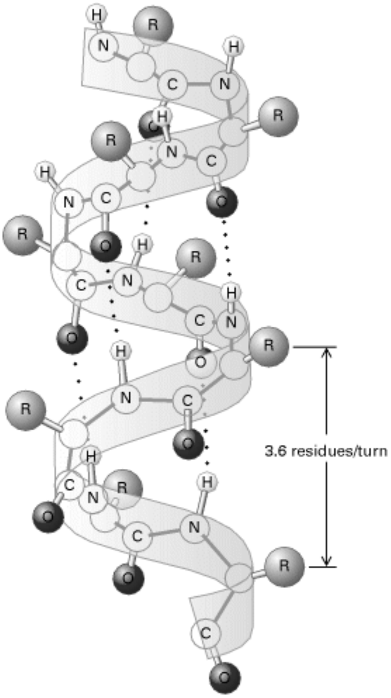

Figure 1. α-helix

β-sheet

The second major structural element found in globular proteins is the β-sheet. The basic unit is the β-strand in which the polypeptide is almost fully extended. This conformation is only stable when incorporated into larger β-sheets since there are no interactions between atoms close in the covalent structure. On the other hand, in the β-sheet there are hydrogen bonds formed between C=O groups on one β-strand and NH groups on an adjacent β-strand. The β-strands can interact in two ways to form a β-sheet. Either the amino acids in the aligned β-strands run in the same direction, in that case the sheet is described as parallel, or the amino acids in successive β-strands can have alternating directions, in which case the β-sheet is called antiparallel. Each of the two ways has a distinct hydrogen bonding pattern, see figure 2. Side chains from adjacent amino acids of the same strand protrude from the β-sheet in opposite directions and do not interact with each other, but they have interactions with the backbone and the side chains of neighboring strands.

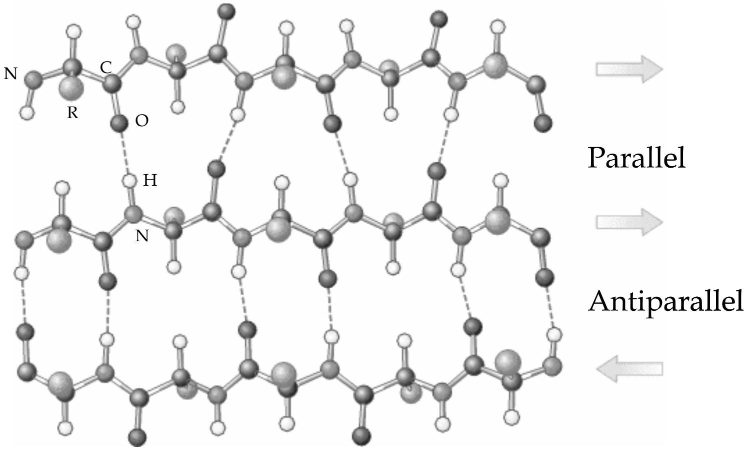

Figure 2. Parallel and antiparallel β-sheets.

PROTEIN FOLDING AND MISFOLDING

The dogma of protein folding, based on the work of Christian Anfinsen some 50 years ago (Anfinsen, 1973), is that all the information required for a protein to fold into its proper three-dimensional structure (and hence the functional form) resides within its amino acid sequence. The native state of a protein is a well ordered system and proteins denature in an all-or-none fashion. This is due to the cooperativity of the interactions that hold the protein together, such as hydrogen bonds, van der Waals interactions, electrostatic- and hydrophobic interactions. Many interactions are formed when a protein folds and still the native state is only favored by 5-15 kcal/mol of free energy under physiological conditions (Almstedt et al., 2004; Almstedt et al., 2008; Creighton, 1990). This is because the free energy (G) is balanced by enthalpic (H) and entropic (S) terms:

$$\Delta G = \Delta H - T\Delta S$$

The decrease in enthalpy compensates for the loss of entropy when a protein folds. The result is that proteins are metastable and this is important for the protein function, which often requires a dynamic structure, and also for the turn-over of proteins in the cell.

Even if a protein successfully reaches its biologically active state, this does not always mean the end-point of its folding/unfolding life. Many proteins go through cycles of unfolding and refolding due to a variety of causes that include transport across a membrane, cellular secretion or exposure to stress conditions (*e.g.* changes in pH or temperature). As a result, the probability for a protein to misfold is relatively high and the process of protein folding must be tightly controlled to ensure that it proceeds correctly. The failure of a protein to fold correctly can have devastating consequences: it is now recognized that protein misfolding cause a variety of our most feared diseases.

Protein folding models

Both the thermodynamic and the kinetic requirements must be met for a protein to fold. This means that the native state has to be thermodynamically stable and the protein must rapidly find the native state. If a protein searches through all possible conformations in a random fashion until it finds the conformation with the lowest free energy it will take an enormous amount of time. Imagine a polypeptide chain with 100 residues and every residue has 2 possible conformations. The protein has 2^{100} or 10^{30} possible conformations, and if it converts one conformation into another in the shortest possible time (maybe 10^{-11} s) the time required is 10^{11} years. A protein however reaches its native fold in 10^{-3} to 10^{3} s both *in vitro* and *in vivo*. These contradicting facts were remarked upon in 1969 by Cyrus Levinthal, and is therefore known as the Levinthal paradox (Levinthal, 1969).

A so called "new view" of the protein folding kinetics has emerged since the middle of the 1990s, made possible from both experimental and theoretical advances (Baldwin, 1994, 1995; Dill and Chan, 1997; Dinner et al., 2000; Wolynes et al., 1995). The main experimental advances have been in methods like high-resolution hydrogen exchange, mass spectrometry, NMR, mutational studies and laser triggered methods that have made studies of the very early events in protein folding possible down to the atomic level (Dill and Chan, 1997; Dinner et al., 2000). The theoretical models that have contributed to the new view are statistical mechanics models. These are highly simplified due to the computational limitations, and are most often lattice based, but even though they lack atomic detail they include the main ingredients of proteins; chain connectivity, flexibility, excluded volume, and sequence dependent intrachain interactions (Bryngelson et al., 1995; Chan and Dill, 1996). It is necessary to find progress variables for monitoring the folding reaction. One parameter sometimes used is the radius of gyration, R_g, but this is not always a useful tool due to little or no change in R_g when a system goes from a compact globule to the native state. A more useful progress variable to monitor the folding progression is the fraction of native contacts Q_0, which goes from 0 in the unfolded states to 1 in the native state, see figure 3. Because the energy and number of conformations accessible to the protein decrease as the number of native contacts increases, the term "folding funnel" and "energy landscape" has been introduced to describe the folding (Dill and Chan, 1997; Dobson et al., 1998). The vertical axis of a funnel represents the internal free energy of a given chain conformation and the lateral axes represent the conformational coordinates. Energy landscapes can have many different shapes and have many "hills" which represents the high energy conformations that sometimes has to be passed to reach the native state.

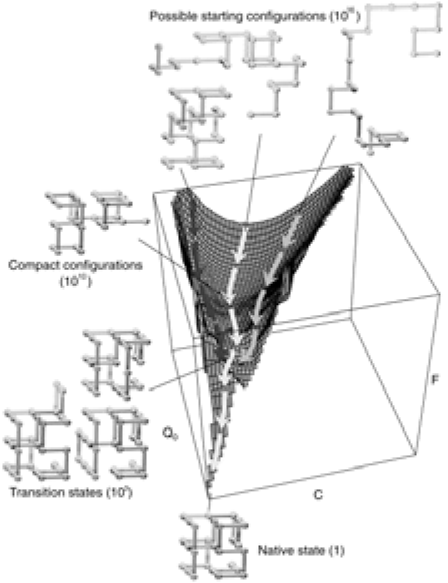
Possible starting configurations (10[illegible])
Compact configurations (10[illegible])
Transition states (10[illegible])
Q_0
F
C
Native state (1)

Figure 3. Free energy (F) surface as a function of native contacts (Q_0) and total number of contacts (C). The structures illustrates various stages of the reaction. From (Dinner et al., 2000).

The folding of a protein does not start from one specific denatured conformation, but rather a distribution of states, called ensemble, with different global and local properties (Shortle, 1996; Smith et al., 1996). When folding conditions are initiated the chain usually collapses rapidly to an ensemble of conformations which have about 60% of the total number of possible contacts (C), but only about 25% of the native contacts (Q_0), see figure 3, (Dobson et al., 1998; Sali et al., 1994). After the collapse the chain encounters the rate limiting stage in the folding reaction, which is the random search through the compact transition states that lead to the native state. The protein folding transition state is not well defined, but can be many different chain conformations. Non-native contacts must be disrupted to allow formation of the native state, but this does not necessarily mean a full opening of the chain, just a few contacts may have to be broken for the chain to continue down towards the native state (Camacho and Thirumalai, 1993; Chan and Dill, 1994).

The solution to the Levinthal paradox that has emerged from lattice models in the new view of looking at protein folding is that only a small number of conformations have to be sampled for a protein to go from random coil to native state, because the nature of the folding funnel restricts the search and there are many transition state conformations. Every individual polypeptide chain is likely to follow different paths down the funnel, in which the native contacts are formed in different orders. The different conformations tend to have more contacts in common as the native state is approached. Because the shape of the funnel is encoded in the amino-acid sequence the natural selection has enabled proteins to evolve so they can fold fast and efficiently.

Protein aggregation

The off-folding pathway has been described to comprise two distinct routes by which aggregation of the protein may proceed, the formation of disordered, amorphous aggregates or ordered amyloid fibrils. Which off-folding pathway the protein stumbles down is thought to be decided by the rate at which a protein unfolds and aggregates, its amino acid sequence, and the nature of the intermediates that are formed (Dobson, 2003; Stefani and Dobson, 2003).

A disordered aggregate is the result from the rapid unfolding and aggregation of intermediately folded proteins, in which the monomers add up to the growing aggregate through a random process. This leads to an amorphous aggregate that eventually becomes too large that it precipitates. This type of aggregation is often responsible for proteins "falling out" of solution when changing buffer conditions and it is also believed to be the underlying mechanism behind inclusion body formation during recombinant protein expression in bacterial cells. However, under normal circumstances in the cell, amorphous aggregation is not a problem since the cell has defense machinery that is well equipped to detect and dispose of them before they precipitate.

In contrast to the formation of disordered protein aggregates, aggregation can occur through a highly ordered, nucleation dependent process, in which the partially folded protein associates to form a stable nucleus. This nucleus acts as a template for other intermediates to add to the growing thread of aggregated protein, called a protofibril. The addition of intermediates to the protofibril leads to the formation of a highly structured, insoluble form of aggregate called amyloid fibril, see figure 4. The formation of the nucleus is the rate determining step, and this is seen in the lag phase in amyloid fibril formation kinetic curves.

Recently it has been shown that inclusion body formation in bacterial cells is a process where amyloid-like aggregates form (Wang et al., 2008). Hence the view of amyloid being distinct from amorphous aggregates should be questioned and are likely highly related processes (Almstedt et al. Paper IV).

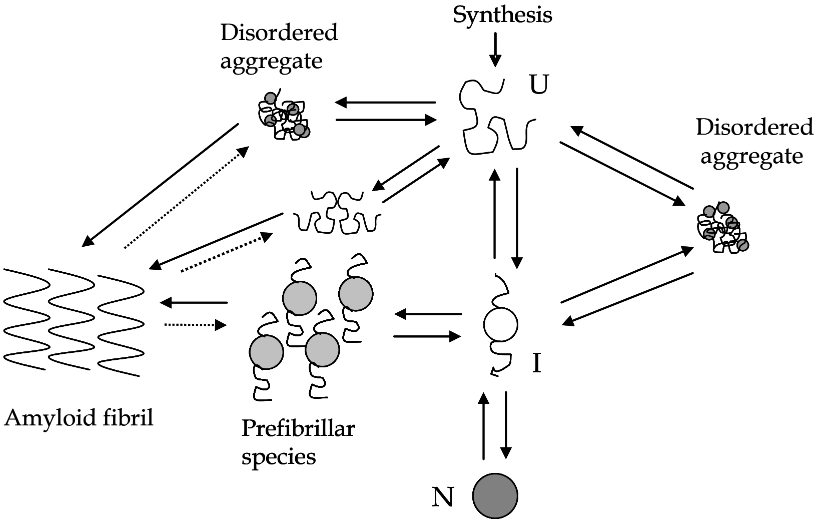

Figure 4. Schematic representation of some of the states accessible to a polypeptide chain following its synthesis. The protein is assumed to fold from its highly disordered state (U) through a partially folded intermediate (I) to its globular native state (N). The unfolded and intermediate states can form aggregated species that often appear disordered whereas amyloid fibrils can form through a highly ordered nucleation dependent mechanism and can only grow in two directions. Amyloid fibrils can also nucleate from disordered aggregates.

Amyloid fibrils

Amyloid fibril formation is associated with a wide range of diseases and many believe it to be linked to the onset and progress of the diseases (Pepys, 2006). The disease-related proteins found as fibrillar aggregates *in vivo* does not share sequence or structural similarities in their native states. Furthermore, the amyloid fibril conformation has been found to be accessible to a diverse range of proteins, so it is now thought to be a generic structural form that all proteins can adopt given the appropriate conditions (Chiti et al., 1999; Dobson, 1999; Stefani and Dobson, 2003; Wetzel, 2002). The overall stability of the fibril is due to intermolecular hydrogen bonding between the amide and carbonyl groups of the polypeptide backbone, and this is thought to be the reason why all fibrils share this morphology, since all proteins have the peptide backbone in common. However, the propensity for a given protein or peptide to form fibrils varies with its amino acid sequence and some regions of a protein are more aggregation-prone than others.

Mature fibrils are usually made up by 2-6 protofilaments plaited together to form a rope-like fiber, 5-10 nm in diameter and up to a few microns in length (Jimenez et al., 1999; Jimenez et al., 2002). The fibrils formed are often unbranched, extremely stable and resistant to degradation by proteases and denaturants (Jimenez et al., 2002; Serpell et al., 2000). These properties are thought to be the reason why cells have difficulties to get rid of the fibrils once they have been formed.

Amyloid fibrils share a characteristic cross β-sheet array, so called because of individual fibrils are made up of β-sheets which lie perpendicular to the core axis of the fibril and which stack together to form an individual filament, see figure 5A. This results in a characteristic cross formed by the meridional and equatorial reflections in X-ray diffraction studies, representing the hydrogen bonding distance between adjacent β-strands that make up a β-sheet and the distance between β-sheets respectively, the former of ~4.5 Å and the latter of ~9-11 Å, see figure 5B.

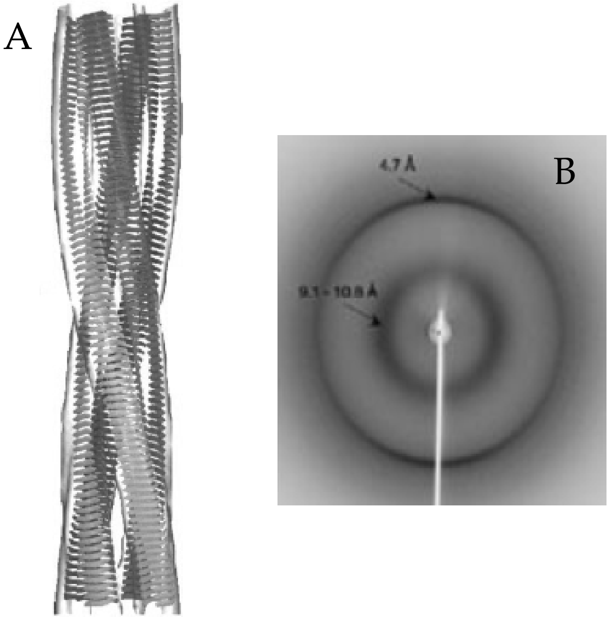

Figure 5. A) A schematic view of an amyloid fibril formed from insulin (Jimenez et al., 2002). The four protofilaments are colored separately. **B)** X-ray fiber diffraction of amyloid fibrils showing the diagnostic meridional and equatorial reflections which forms the cross β-sheet pattern (Ecroyd and Carver, 2008).

The amyloid fibrillation process is promoted when the protein is exposed to various stress factors, such as lowered pH, presence of denaturants, elevated temperatures and/or hydrophobic surfaces (Fink, 1998; Sluzky et al., 1991). It has also been shown that agitation can speed up the fibrillation process, but the reason why is not clear. The increase of air-water surface formed by agitation can affect the fibrillation rate since the interface act like a hydrophobic surface, which is known to induce fibril formation (Nielsen et al., 2001; Sluzky et al., 1991). The air-water interface is denaturing; it has been shown that β-lactoglobulin was severely destabilized (ΔΔG = 12 kcal/mol) at the air-water interface compared to in solution (Perriman et al., 2007). The agitation is also thought to increase the number of fibril ends by amyloid fragmentation and also to increase the collision rate between oligomeric species and/or the fibril ends (Collins et al., 2004b; Serio et al., 2000). The amyloid fibrillation process is usually divided into three parts, which can clearly be seen in a fibrillation kinetics curve, see figure 6. First there is a lag phase in the early stages of the fibrillation process when oligomeric species are thought to form and these do not bind to the traditional fluorescent dyes that are used to detect fibrils. This phase is followed by the elongation phase where fibrils are formed and the fluorescence signal is increasing until the third phase (the equilibrium phase) in the process is reached.

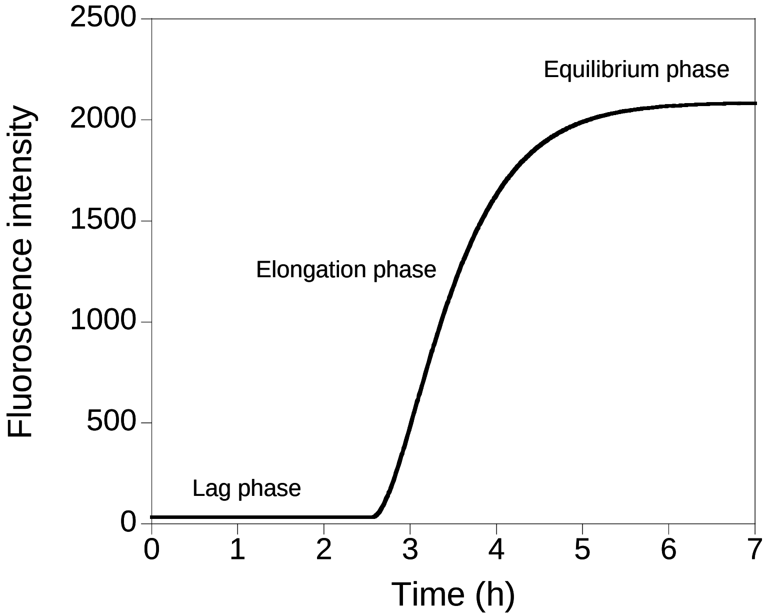

Figure 6. Fibrillation kinetic curve from fibrillation of ^{His}HuPrP$_{90\text{-}231}$ in 50 mM phosphate buffer, 100 mM NaCl, 50 mM KCl, pH 7.3, at 37°C with agitation. From Almstedt et al. Paper IV.

In many diseases, the amyloid fibrils assemble into tangled plaques, which is the hallmark of most neurodegenerative diseases and the site at which the toxic effect of fibril formation is most evident. Although there are obvious negative effects of extracellular amyloid plaque deposition (Pepys, 2006; Tan and Pepys, 1994), recent studies show that it is primarily the soluble, pre-fibrillar oligomers, which are formed during the early stages of fibril formation, that are the most cytotoxic species in neurodegenerative diseases mainly as deduced from studies in cell culture (Bucciantini et al., 2002; Conway et al., 2000; Lambert et al., 1998; Simoneau et al., 2007; Sorgjerd et al., 2008; Stefani and Dobson, 2003). The nature of this pathogenic species and the mechanism by which the aggregation process causes cell damage is not known.

THE MODEL PROTEINS

Carbonic Anhydrase

The enzyme carbonic anhydrase (CA) catalyses the reaction in which carbon dioxide is hydrated into bicarbonate:

$$CO_2 + H_2O \leftrightarrow HCO_3^- + H^+$$

This reaction is involved in many different physiological processes for example respiration, bone resorption and acid-base balance. Carbonic anhydrases are divided into different families or classes (α, β, γ, δ and ε) who are genetically unrelated. In mammals only the α-form is present and in humans there are 10 enzymatically active isoenzymes described with different catalytic activity, cellular location and tissue distribution and three non-catalytic isoforms with unknown function (Lehtonen et al., 2004; Shah et al., 2000). Of all enzymatic reactions studies so far the enzyme human carbonic anhydrase II (HCA II) is one of the most efficient known with a turnover rate of approximately 10^6 s^{-1} (Lindskog, 1997; Steiner et al., 1975).

Human carbonic anhydrase II

HCA II has a molecular weight of 29100 Daltons and consists of 259 amino acids. The structure has been determined to a resolution of 1.54 Å (Hakansson et al., 1992) and is dominated by a 10-stranded β-sheet that divides the protein in two parts, see figure 7. One part contains an extensive hydrophobic core and the other part contains a 24 residue N-terminal mini domain and the active site.

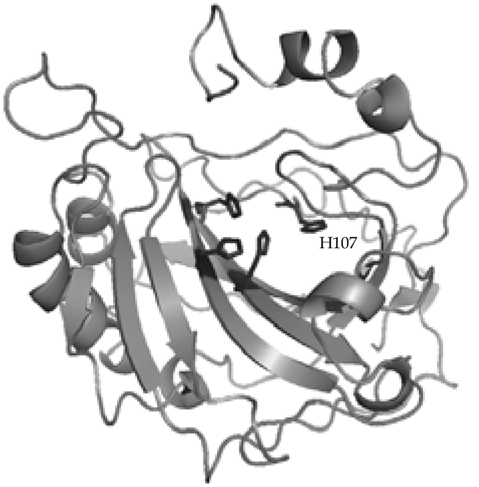

Figure 7. Structure of HCA II with the side chains of H94, H96, H119 and H107 shown as stick models. PDB code 1CA2.

The active site is situated in a 15 Å deep cone shaped cavity in the enzyme and at the bottom of this funnel a Zn^{2+} ion is coordinated by three histidines (His-94, 96 and 119) and a water molecule, see figure 8. The catalytic mechanism starts with an attack from a zinc-bound OH^- on a CO_2 molecule to form a zinc-bound HCO_3^- ion. This ion is then displaced by a H_2O molecule, and the zinc-bound OH^- is regenerated by the rate limiting transfer of a water proton to His-64 which shuffles the proton to a buffer base (Tu et al., 1989). The C-terminal of the protein forms a well defined knot topology, *i.e.* the end of the protein (β-strand 9) is inserted between β-strand 8 and 10 (Freskgard et al., 1991).

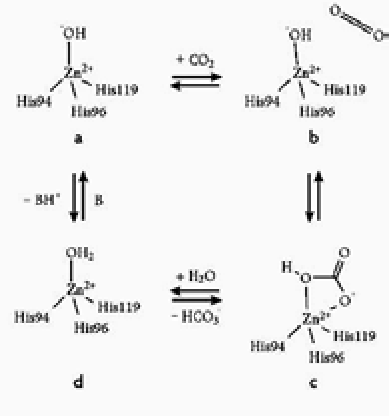

Figure 8. Schematic figure showing the catalytic mechanism for HCA II. Carbon dioxide is hydrated into bicarbonate.

The wild-type enzyme has a cysteine residue in position 206, which has been replaced by a serine to obtain the pseudo wild-type of the enzyme (HCA $\mathrm{II}_{\mathrm{pwt}}$). This variant is indistinguishable from the wild type regarding activity and stability (Martensson et al., 1992; Martensson et al., 1993), and a majority of our folding work has been performed on this pseudo wild-type.

The protein contains seven tryptophan residues well distributed through the protein structure, which makes monitoring changes in tertiary structure possible by intrinsic fluorescence and circular dichroism. In GuHCl the protein unfolds via two well separated transitions, indicating the presence of a stable folding intermediate with residual structure. Due to the cooperativity of the folding reaction stable folding intermediates are rare and make HCA II an interesting model system. Measurements have shown that the folding intermediate is of molten-globule type that lacks enzyme activity (Martensson et al., 1992; Martensson et al., 1993; Svensson et al., 1995). This molten globule state is also very aggregation-prone, and the aggregation process is very specific and comprises the central hydrophobic β-strands 4 and 7 (Hammarstrom et al., 2001a; Hammarstrom et al., 2001b; Hammarstrom et al., 1999).

Inhibition and Activation of Carbonic Anhydrase

The carbonic anhydrase reaction is involved in many physiological and pathological processes, including respiration and transport of CO_2 and bicarbonate between metabolizing tissues and lungs; calcification; electrolyte secretion in various tissues and organs; bone resorption; and pH and CO_2 homeostasis (Ridderstrale and Hanson, 1985; Sly et al., 1983; Sly et al., 1985; Supuran, 2008). Many of the carbonic anhydrase isozymes are important therapeutic targets and there are two main classes of Carbonic Anhydrase inhibitors (CAIs); the metal-complexing anions and aromatic and certain heterocyclic sulfonamides. The catalytic reaction is inhibited by the anions through displacement of the zinc bound H_2O molecule and preventing the formation of the OH^- ion (Lindskog, 1997). The sulfonamides bind to the metal ion as anions via the nitrogen atom of the sulfonamide group. There are many crystal structures of CA-sulfonamide complexes available, and in all of these the mode of binding of the sulfonamide group are the same, see figure 9 (Hakansson and Liljas, 1994; Weber et al., 2004; Vidgren et al., 1990).

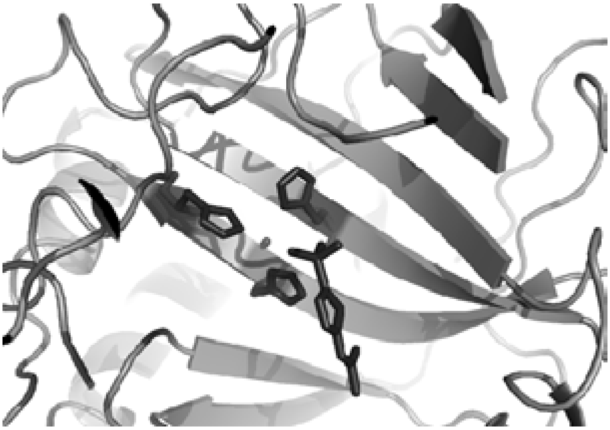

Figure 9. Crystal structure of the complex between HCA II and the inhibitor acetazolamide. Residues H94, H96, H119 and acetazolamide are shown as stick models. PDB code 1YDA.

Even though the field of CAIs is extensively studied, the field of CA activators (CAAs) still remains largely unexplored. However, it has recently been shown that the activator phenylalanine, when administered to experimental animals, produces a relevant pharmacological enhancement of synaptic efficiency (Sun and Alkon, 2002). It has been proved that the activator binds within the active-site cavity at a site distinct from the inhibitor or substrate binding-sites, to facilitate the rate determining step of proton transfer. This has also been shown for the activator histidine, see figure 10 (Temperini et al., 2006a, b).

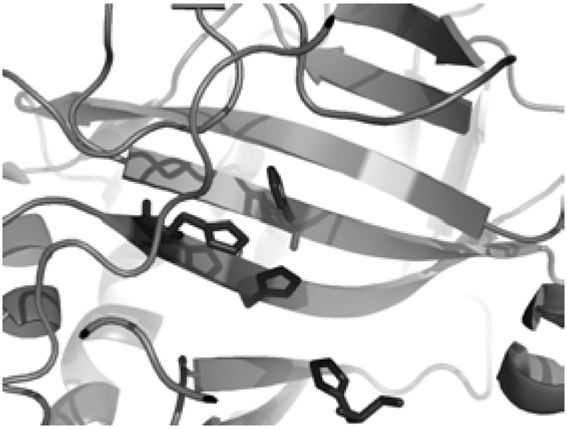

Figure 10. Crystal structure of the complex between HCA II and L-His. Residues H94, H96, H119 and L-His are shown as stick models. PDB code 2ABE.

Human Prion Protein

PrP^C (C stands for cellular) is encoded by *PRNP*, a small, single copy housekeeping gene on chromosome 20, which is expressed at high levels in neurons. Human PrP^C is synthesised as a 253 amino acid polypeptide chain from which the first 22 amino acids (signal peptide) are cleaved shortly after the translation is finished. PrP^C has a ~100 amino acids long flexible, random coil N-terminal domain and a C-terminal globular domain composed of residues 121-231. The globular domain is arranged in three helixes (amino acids 144-154, 173-194 and 200-228) and two β-strands (amino acids 128-131 and 161-164), see figure 11 (Linden et al., 2008). A single disulfide bond is found between cysteine residues 179 and 214, connecting α-helix 2 and 3. In the unstructured N-terminal domain (amino acids 23-120) there are five highly conserved, repeating octapeptide domains that bind metal ions, including Cu^{2+}. There is a common polymorphism (methionine or valine) in position 129, which plays an important role in different prion diseases (Brown et al., 1997; Hornshaw et al., 1995; Stockel et al., 1998), see the chapter Human Prion Diseases.

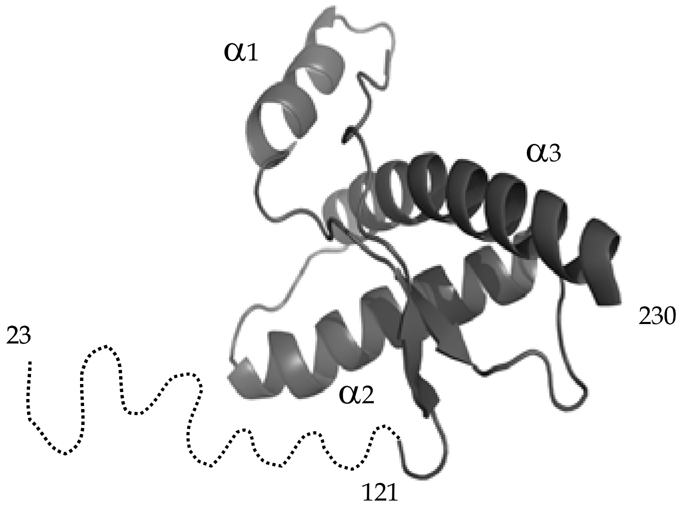

Figure 11. Cartoon of the three dimensional NMR-structure of human prion protein, $HuPrP_{23\text{-}231}$.
The flexible disordered "tail" of residues 23-120 represented by dots.
PDB code 1QLX From (Zahn et al., 2000).

The PrP^C polypeptide is synthesized in the endoplasmic reticulum, ER, processed in the Golgi apparatus and transported in its mature form to the cell membrane where it localizes in lipid rafts (Kovacs and Budka, 2008). Post-translational modifications include removal of the GPI signal peptide and adding a C-terminal glycosylphosphatidylinositol (GPI)-anchor at residue 230, which facilitates linkage to the cell membrane. Two N-linked glycosylation sites are located at residues 181 and 197, and the full length PrP^C is found in non-, mono- or diglycosylated forms. The nearly identical structures of both recombinant PrP^C and glycosylated PrP^C isolated from calf brain indicate that neither the glycosylations nor the GPI anchor affects the structural features (Hornemann et al., 2004).

The functional roles of PrP^C have yet to be determined. Surprisingly, the first knockout mouse lacked the disease phenotype (Bueler et al., 1992). This result suggested that either PrP^C is unnecessary for normal development, or that its absence is compensated by a redundant protein which maintains an important phenotype. Nevertheless, the *PRNP* is a very conserved gene and PrP^C is highly expressed in the mammalian brain. The main hypothesis is that the prion protein is a dynamic cell surface platform for the assembly of signaling molecules and thereby involved in selective molecular interactions and transmembrane signaling which have wide-range consequences upon both physiology and behavior. It was recently shown that PrP^C is necessary for olfactory behavior and physiology in mice (Le Pichon et al., 2009).

If (and how) copper binding relates to normal PrP^C function and whether it is involved in disease pathogenesis remains unclear. The binding of Cu^{2+} to PrP^C appears to influence cellular resistance to oxidative stress, but the mechanism behind this still remains unknown (Linden et al., 2008; Perera and Hooper, 2001).

PROTEIN MISFOLDING DISEASES

There are several well-known diseases that are due to aberrant protein folding, see table 1. These types of diseases can be divided into three main categories:

1. Loss-of-function diseases
2. Gain-of-toxic-function diseases
3. Infectious misfolding diseases

The *loss-of-function folding diseases* are often inherited in a recessive manner. The protein involved in the disease is mutated in a way that causes the loss of its function, either due to incorrect folding or an early termination of the protein transcription resulting in degradation of the product. The fact that most of these diseases are recessive is due to the high specific activity presented by proteins, allowing them to compensate for the low abundance of the active protein occurring when you have one allele coding for the correct form and the other allele coding for a mutated non-active form.

Many well known diseases are in this category, for example hemophilia, cystic fibrosis, phenolketonuria and cancer (Gregersen, 2006). In many cases the underlying protein is hard to study and only limited information can be obtained due to the difficulty of expressing and studying these proteins *in vitro*.

In the case of *gain-of toxic-function diseases* the situation is a little different. Here the proteins involved misfold and adopt a structure toxic to the cell. The mechanism behind this toxicity is not yet fully understood, but there are several proposed models, such as the formation of pores in the cell membrane or activation of surface receptors (Sousa et al., 2000; Volles and Lansbury, 2003). In recent models it is thought that misfolded proteins form soluble oligomeric assemblies that mediate toxic effects on the cell.

The *infectious misfolding diseases* is the smallest group of diseases. The only protein known today that has the ability to transmit infectivity is the prion protein. In 1982 Stanley Prusiner coined the term "prion" to distinguish the proteinaceous infectious particle that cause for instance scrapie in sheep (Prusiner, 1982). A protein was found that was unique for scrapie-infected brains and later also for Bovine Spongiform Encepalopathy in cattle and Creutzfeldt-Jakob disease in humans, and was later named prion protein and abbreviated PrP. (Prusiner, 1994).

	Disease	Precursor protein
Loss-of-function	Cancer	P53 tumor suppressor
	Cystic Fibrosis	CFTR
	Carbonic Anhydrase II Deficiency Syndrome	HCA II
Gain-of-toxic function	Alzheimers disease	Aβ-protein
	Type II diabetes	IAPP
	ALS	Superoxide dismutase
	Parkinson's disease	α-synuclein
Infectious-misfolding	Creutzfeldt-Jakob disease	Prion protein
	BSE	Prion protein
	Kuru	Prion protein
	Scrapie	Prion protein

Table 1. Examples of misfolding diseases and their underlying proteins.

Carbonic Anhydrase II Deficiency Syndrome

In 1983 deficiency of HCA II was identified as the primary defect causing osteopetrosis (excessive bone growth) with renal tubular acidosis (RTA) and cerebral calcification (Sly et al., 1983). The disease carbonic anhydrase II deficiency syndrome (CADS) is also known as marble brain disease or Guibaud-Vainsel syndrome. This syndrome caused by the lack of active HCA II is quite rare, and most cases has been found in families where some inbreeding has occurred (Sly and Hu, 1995). The disease is usually discovered late in infancy or early in childhood through developmental delay, short stature, fractures due to brittle bones, weakness, cranial nerve compression, dental malocclusion, and/or mental sub normality.

Osteopetrosis is caused by a disturbance in the osteoclasts when no active HCA II is present. Osteoclasts dissolve bone mineral during the resorption process by targeted secretion of protons into a resorption lacuna (one of the numerous minute cavities in the substance of bone). Proton secretion into the lacuna leads to local acidification and dissolution of bone mineral. The proton secretion and mineral dissolution is dependent of the activity of the ATP-dependent proton pump at the ruffled border membrane of the osteoclasts (Sundquist et al., 1990). Osteoclasts contain a large amount of mitochondria required to produce enough ATP for proton secretion. This produces CO_2 that is converted into bicarbonate and protons via HCA II to fulfill the need of H^+ for the proton pump. Thus protons for acid production in osteoclasts are most probably provided by HCA II (Hentunen et al., 2000).

The RTA usually includes both *proximal* and *distal* components. In the *proximal* tubule the bicarbonate reclamation occurs. This is a two-step process and it involves both HCA IV in the first step and then HCA II in the second step. In the proximal tubule cytosolic HCA II disperses the accumulating OH^- generated by the H^+ transporters at the cytoplasmic side of the membrane. By catalyzing the formation of HCO_3^- from CO_2 and OH^-, rate limiting inhibition of these H^+ transporters can be prevented. In the *distal* human nephron there are HCA II-rich cells specialized in secreting H^+. As in the bone-resorbing reaction it is an ATPase that is secreting H^+ and thereby generates OH^- which requires a working HCA II to maintain the pH balance (Swenson, 2000). If HCA II is not present or inactivated the result will be elevated urine pH, which is found in the CADS patients.

Although CA II has been detected in epithelial cells of the choroid plexus, oligodendrocytes and astrocytes on histochemical analyzes of mammalian brain tissue, the mechanism behind the cerebral calcification found in CADS still remains unclear.

The first HCA II mutation to be characterized was from a Belgian patient who was homozygous for a histidine to tyrosine change at the highly conserved histidine at position 107 (Venta et al., 1991). The three affected sisters in the American family in which CADS was first reported were also found to have this mutation (Roth et al., 1992) and it has also been found in Italian and Japanese patients (Soda et al., 1996; Sundaram et al., 1986). Neither the Belgian patient or the American patients were mentally retarded, and it has been speculated that a small amount of residual HCA II activity allows them to escape mental retardation (Roth et al., 1992). This mutation has been the focus for *in vitro* studies (Almstedt et al., 2004; Almstedt et al., 2008; Roth et al., 1992) and it is the most studied mutant causing this disease.

All CADS patients discovered to date have been found to have mutations in the coding sequence or splice junctions of the CA2 gene. The mutations known to cause the disease are shown in table 2.

Mutation base change	Predicted consequence	Ethnic group	Reference
c.82C>T	Q28X	Turkish	(Shah et al., 2004)
c.99delC	I33fsX	Italian	(Hu et al., 1997)
c.120T>G	Y40X	Japanese	(Soda et al., 1995)
c.142_145delTCTG	S48fsX	American	(Hu et al., 1997)
c.145_148delGTTT	V49fsX	American	(Shah et al., 2004)
c.157delC	Q53fsX	Brazilian	(Hu et al., 1997)
c.191delA	H64fsX	Egyptian	(Hu et al., 1997)
c.220_221delCA	Q74fsX	Ecuadorian	(Shah et al., 2004)
c.232+1G>A	Splicing mutation	Arabian	(Hu et al., 1992)
c.275A>C	Q92P	Gypsy (Czech)	(Hu et al., 1997)
c.280C>T	H94Y	Canadian	(Shah et al., 2004)
c.290G>A	Y96X	Italian	(Shah et al., 2004)
c.319C>T	H107Y	Belgian Italian Japanese	(Venta et al., 1991) (Roth et al., 1992) (Soda et al., 1996)
c.430G>C	G145R	Canadian	(Shah et al., 2004)
c.505delA	K169fsX	Afghani	(Shah et al., 2004)
c.507-1G>C	Splicing mutation	German	(Roth et al., 1992)
c.535_536insGT	D179fsX	Italian	(Shah et al., 2004)
c.621delC	W208fsX	Turkish	(Shah et al., 2004)
c.630_641del12insCACA	L211fsX	Irish traveler	(Shah et al., 2004)
c.663+1G>T	Splicing mutation	Italian	(Hu et al., 1997)
c.679delA	K227fsX	Caribbean Hispanic	(Hu et al., 1994)
c.696_697delGG	E233fsX	Indian	(Shah et al., 2004)
c.753delG	N253fsX	Mexican	(Hu et al., 1997)

Table 2. Mutations causing Carbonic Anhydrase II Deficiency

Transmissible Spongiform Encephalopathy

Transmissible spongiform encephalopathy (TSE) or prion diseases are fatal neurodegenerative diseases in human and animals that originate spontaneously, genetically or by infection. The pathogenesis of TSE is linked to the simultaneous expression of the host-encoded prion protein (PrP^C) and the conversion into the disease-causing isoform PrP^{Sc} (Collins et al., 2004a; Kovacs and Budka, 2008; Simoneau et al., 2007; Stohr et al., 2008). Several mechanistic models have been reported for this conversion, but most data supports the model of the seeded polymerization (Harper and Lansbury, 1997). The transition of PrP^C into PrP^{Sc} can be induced *in vivo* either by an infection with prions, by spontaneous conversion or by mutations in the PrP sequence. No matter what caused the conversion, the conformation change of PrP^C into PrP^{Sc} results in a fundamental change in its biophysical properties. While PrP^C is rich in α-helical secondary structure, soluble, membrane bound and non-infectious, PrP^{Sc} is β-sheet-rich, aggregated and infectious. Proteinase K digests PrP^C completely but cleaves PrP^{Sc} specifically at amino acid 89 or 90, leaving the C-terminal part intact (residues 90-231).

Human TSEs include sporadic Creutzfeldt-Jakob disease (sCJD), variant CJD, iatrogenic CJD, inherited prion disease and kuru.

Sporadic CJD

Sporadic CJD (sCJD) is the most common human prion disease and the sporadic form accounts for about 85% of the cases. It occurs throughout the world with no seasonal or geographical clustering. The disease affects men and women equally and the average age of onset is about 60 years, it is rare in people under the age of 40 or over the age of80 years (Brown et al., 1994; Ladogana et al., 2005; Linsell et al., 2004). The disease typically presents a rapidly progressive dementia, often accompanied by cerebral ataxia and myoclonus (muscle twitching), the median time to death from onset is only 4-5 months, and 90% of the patients are dead within one year (Johnson and Gibbs, 1998). The pathological findings are limited to the brain and spinal cord. There is neuronal loss and vacuolization within cell bodies that gives a spongiform appearance to the cortex and deep nuclei. The mode of infection for this disease is unknown. Exposure to people with the illness does not seem to increase the risk, although it is transmissible both to humans and primates through transplantation or experiment, see Iatrogenic CJD below.

Variant CJD

The appearance of a novel human prion disease, variant CJD (vCJD), in the UK from 1995 and onwards, (Will et al., 1996), and the confirmation that this is caused by the same prion strain that cause BSE (mad cow disease) in cattle has led to a concern that exposure to the epidemic of BSE poses a threat to public health both in the UK and other countries. The extremely varied and prolonged incubation time for the disease when transmitted between species means that it will be years before the dimension of a human epidemic can be predicted. In the meantime we have to face the possibility that people incubating the disease can pass it onto others via blood transfusion, tissue and organic transplantation and other iatrogenic routes (Collinge, 1999).

The duration of the disease is longer compared to sCJD with mean patient survival times of about 14 months (Wadsworth and Collinge, 2007), and in mean age of onset the two types of CJD also differ; the mean age of onset in vCJD is only 26 years (Spencer et al., 2002). The early clinical presentations consist of behavioral and psychiatric disturbances, peripheral sensory disturbance and cerebral ataxia.

So far only human BSE infection has been found in people who are homozygous for methionine in position 129, MM. It remains unclear if people with the other *PRNP* codon 129 genotypes, VV and MV, will get the disease after longer incubation time after infection with BSE prions, or if they are protected from the disease by their genotype. A comparison of sCJD and vCJD is shown in table 3.
There are reports of blood transfusion derived transmission from human to human of vCJD in 129 MV carriers (Wroe et al., 2006).

Clinical features	**Variant CJD**	**Sporadic CJD**
Mean age of onset	26 years	60 years
Length of survival	14 months	4 months
Early psychiatric symptoms	Common	Unusual
Dementia	Commonly delayed	Typically early
Histopathology of brain	Many florid plaques	No amyloid plaques
Polymorphism at codon 129	All homozygotes (M/M)	Homozygosity and heterozygosity

Table 3. A comparison between sCJD and vCJD. From (Johnson, 2005)

Inherited prion disease

Traditionally the inherited prion diseases are classified by the presenting clinical syndrome, falling into three different main divisions either of familial CJD, Gerstmann-Sträussler-Scheinker Syndrome (GSS) or Fatal Familial Insomnia (FFI). All are inherited in an autosomal dominant pattern. How the mutations in the *PRNP* gene cause prion disease has yet to be elucidated, but it is thought that in most cases the mutation leads to an increased probability of PrP^C to PrP^{Sc} conversion. Over 30 pathogenic mutations in the *PRNP* gene have been described, shown in figure 12 (Collinge, 2001; Wadsworth et al., 2003).

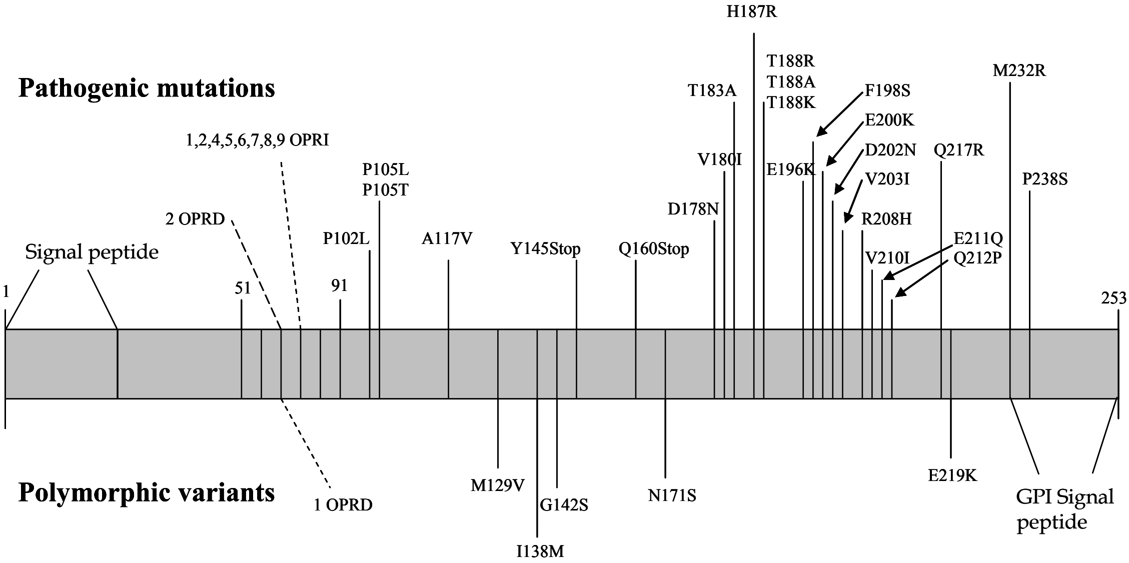
H187R
Pathogenic mutations
T183A
T188R
T188A
T188K
F198S
E200K
M232R
1,2,4,5,6,7,8,9 OPRI
V180I
E196K
D202N
Q217R
P105L
P105T
V203I
P238S
D178N
2 OPRD
R208H
P102L
A117V
Signal peptide
Y145Stop
Q160Stop
E211Q
V210I
Q212P
1
51
91
253
M129V
E219K
Polymorphic variants
1 OPRD
G142S
N171S
GPI Signal peptide
I138M

Figure 12. Pathogenic mutations and polymorphisms in the human prion protein. The pathogenic mutations associated with human prion disease are shown above the human PrP coding sequence. These consist of 1, 2 or 4–9 octapeptide repeat insertions (ORPI) within the octapeptide repeat region between codons 51 and 91, a 2 octapeptide repeat deletion (ORPD) and various point mutations causing missense or stop amino-acid substitutions. Polymorphic variants are shown below the PrP coding sequence. Deletion of one octapeptide repeat is not associated with prion disease in humans.
Redrawn from (Wadsworth et al., 2003)

In general, familial CJD has earlier age of onset than sCJD. Otherwise the clinical symptoms are the same for fCJD and sCJD, and the mutations in the *PRNP* gene were discovered *post mortem* in patients dying from CJD. The most common form of familial CJD results from a mutation at codon 200, E200K.

Patients with GSS share the distinct neuropathological feature of widespread, multicentric amyloid plaques, which are immunoactive for PrP. The typical clinical features are slowly progressive cerebellar ataxia, beginning in the fifties or sixties, accompanied by cognitive decline. The most common mutation giving rise to GSS is P102L, but there are several other mutations known causing this type of prion disease (Kovacs et al., 2005).

Fatal familial insomnia (FFI) has the strangest phenotype for inherited prion diseases. It is dominated by a progressive insomnia, autonomic dysfunction and dementia. The neuropathological changes are localized largely to neuronal loss in the thalamus and there is little vacuolization. The mutation causing FFI is D178N, but this mutation is also seen in fCJD (Nieto et al., 1991). The phenotype of the disease is determined by the polymorphism at codon 129, the FFI patients are homozygous for methionine and the fCJD patients are homozygous for valine or heterozygous. An Italian family suffering from FFI has recently been described in the novel "The family that could not sleep" (Max, 2006) .

Iatrogenic CJD

Iatrogenic CJD (iCJD) has arisen as a complication of neurosurgery, corneal grafts, implantation and therapeutic use of human dura mater, treatment with human cadaveric pituitary growth hormone and stereotactic electroencepalography electrodes. Dura mater and pituitary growth hormone causes account for the most cases (Collins et al., 2004a; Johnson, 2005).

The clinical presentation in iCJD appear to be in relation to the route of exposure, peripheral inoculation and dura mater implants are associated with ataxia, while direct implantation of PrP^{Sc} into the cerebrum is associated with dementia. Also the inoculation time varies with the infection route; direct intracerebral contamination has short incubation times (16-18 months), dura mater grafts have incubation times can be 18 months to 18 years, and the longest delays are found for injections with pituitary hormones (5-30 years) (Collins et al., 2004a; Johnson, 2005; Wadsworth and Collinge, 2007).

METHODS

Site Directed Mutagenesis

To generate the mutants used in this thesis, site-directed mutagenesis in the HCA II_{pwt} gene has been used to replace the chosen amino acid in the produced protein. We used the QuikChange method from Stratagene, a method with high mutation efficiency which does not require isolation of ssDNA. The QuikChange method uses a dsDNA vector with the inserted gene of interest and a complimentary oligonucleotide primer pair that encodes for the desired mutation. The primers are then extended using PCR, and the final product is thereafter treated with DpnI to digest the original methylated plasmids that do not code for the mutant protein. The mutations are verified by DNA sequencing and then transformed into the *E. coli* strain BL21/DE3 for protein expression.

Enzyme Activity

The most sensitive way to follow the folding of an enzyme is to monitor its biological activity. Only a small change in the three-dimensional structure of an enzyme, due to misfolding, unfolding or ligand binding, can have severe effects on its enzymatic capability. The hydration of carbon dioxide, which is catalyzed by HCA II, generates protons which change the pH of the solution. This pH change can easily be monitored if the reaction takes place in a buffer containing a pH-sensitive indicator such as bromthymol blue (BTB) (Rickli et al., 1964).

Fluorescence Spectroscopy

Fluorescence occurs when a fluorescent molecule (typically an aromatic molecule) absorbs light and thereby goes from the ground state to the excited state. This process is usually illustrated by a Jablonski diagram, with a typical example being shown in figure 13. The singlet ground, first and second states are called S_0, S_1 and S_2 respectively. The transitions between the different states are shown by vertical lines to illustrate the almost instant nature of light absorption and emission. The large energy difference between S_0 and S_1 is too large for the thermal population of S_1, and for that reason light must be used to induce fluorescence.

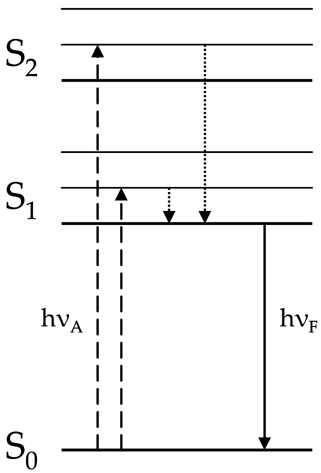

Figure 13. Jablonski diagram showing the energy levels of the ground state S_o and various excited states. After light absorption, where the electrons are lifted from the ground state S_0 to higher energetic excited levels (dashed arrow), vibrational relaxation and internal conversion processes (dotted arrows) take place before light is emitted (solid arrow).

The energy of the emitted light is lower than that of the absorbed light as shown in the Jablonski diagram; this is called the Stokes shift. This energy loss between excitation and emission is observed for all fluorescent molecules in solution (Lakowicz, 2006). The Stokes shift is due to interactions between the fluorophore and its immediate environment. One common cause of the Stokes shift is that when a fluorophore is excited it is usually excited to a higher vibrational level of S_1 or S_2, and the excess vibrational energy is rapidly lost to the solvent when the fluorophore relaxes to the lowest vibrational level in S_1. If the fluorophore is excited to S_2 it rapidly decays into the S_1 state due to internal conversion (Lakowicz, 2006).

Solvent effects can shift the emission to even lower energies due to stabilization of the excited state, see figure 15. This is because the dipole moment is larger in the excited state than in the ground state. The excited state is stabilized by the reorientation of the polar solvent molecules that relaxes around the excited state and thereby lowers its energy. This effect becomes larger as the polarity of the solvent increases, resulting in emission at longer wavelengths. This solvent effect influences fluorophores that intrinsically are more polar than non-polar fluorophores, and it can be used for monitoring the polarity of the solvent surrounding the fluorescent molecule (Bayliss and McRae, 1954).

Fluorophores

Fluorophores are divided into two classes; intrinsic and extrinsic. Intrinsic are those fluorophores that occur naturally and are a part of the protein molecule, and extrinsic are those added to a sample to obtain the desired fluorescence properties. The dominating intrinsic fluorophore in proteins is the tryptophan residue with its fluorescent indole group. Indole absorbs light near 280 nm and emits near 340 nm. The indole group is a solvent-sensitive fluorophore and the emission spectrum of indole is highly sensitive to solvent polarity, and can thereby reveal the location of tryptophan residues in proteins. The emission of a tryptophan residue that is buried in the hydrophobic interior of a protein will emit light of higher energy (blue shift) than that from a surface exposed residue (red shift). This phenomenon is illustrated in figure 14, which shows the shift in emission spectrum of tryptophan residues upon unfolding of a protein. In the folded native state the tryptophan residue is shielded from the solvent but in the unfolded state the tryptophan is exposed to the aqueous phase.

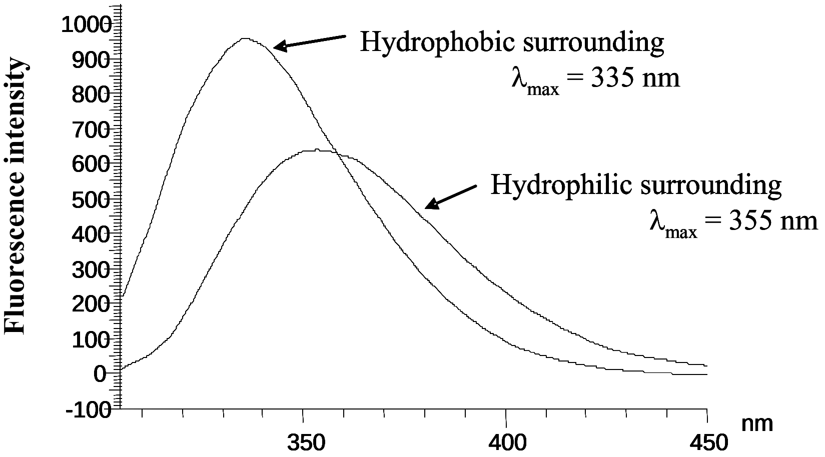

Figure 14. Fluorescence spectra of tryptophan in different surroundings.

Other common mechanisms governing the fluorescence properties of extrinsic fluorophores are internal charge transfer (ICT) including twisted internal charge transfer (TICT) (Rettig, 1986). In ICT and TICT an electron is transferred from an electron donor group (*e.g.* an amino group) to an electron acceptor group (*e.g.* an aromatic system) in the excited dye molecules. For TICT a change in the conformation of the fluorophore, e.g. rotation or twist, is a prerequisite for the electron transfer to take place. The charge separation induced by (T)ICT gives rise to an increased dipole moment of the excited state $S_{(T)ICT}$ compared to S_1, see figure 15. Formation of (T)ICT is favored in polar solvents and results in enhanced solvent relaxation processes and a more pronounced Stokes shift. Additionally, for fluorescent dyes (T)ICT states are in most cases more likely to relax by nonradiative processes than by fluorescence emission, resulting in low fluorescence intensities of the dyes in polar environments (Chang and Cheung, 1990; Das et al., 1992; Hawe et al., 2008).

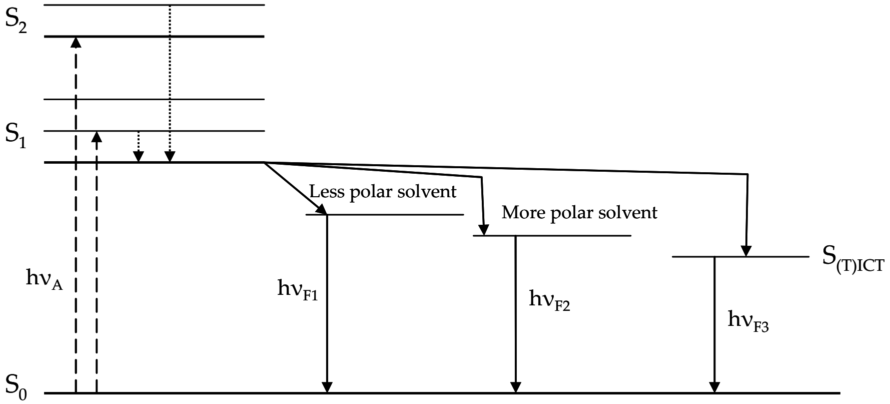

Figure 15. Jablonski diagram for fluorescence with solvent relaxation and internal charge transfer.

Many fluorophores are sensitive to their surrounding environment. The emission spectra and intensities of extrinsic probes are often used to determine the location of the probe on a protein. One of the best known examples is the probe 8-anilino-1-naphtalenesulfonic acid (ANS), see figure 16. ANS is essentially non-fluorescent in aqueous solutions but becomes highly fluorescent in non polar solvents or when bound to proteins and membranes. ANS-type dyes are amphiphatic, so that the non-polar region of the molecule prefers to adsorb onto the non-polar regions of proteins. Since the probe does not fluoresce in the water phase, the emission signal is only from the area of interest, which is the probe binding site on the protein.

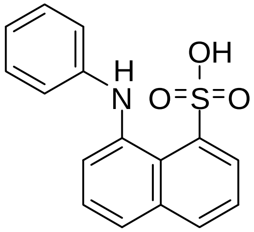

Figure 16. 8-anilino-1-naphtalenesulfonic acid (ANS)

Thioflavin T (ThT, figure 17) is a cationic benzothiazole dye that shows enhanced fluorescence upon binding to amyloid in tissue sections. ThT has been used as histochemical dye to stain amyloid-like deposits in tissues and later for quantification of amyloid fibrils *in vitro* in presence of amyloid precursor proteins and amorphous aggregates (Hawe et al., 2008; Kelenyi, 1967; LeVine, 1999; Naiki et al., 1989; Vassar and Culling, 1959). In the presence of amyloids, ThT exhibits an additional absorption peak at 450 nm and becomes highly fluorescent with an emission maximum at 480 nm, resulting from interactions between ThT and amyloid fibrils on fluorescence. Although it is commonly used for the detection of amyloid fibrils *in vivo* and *in vitro*, not much is known about the mechanism of ThT binding.

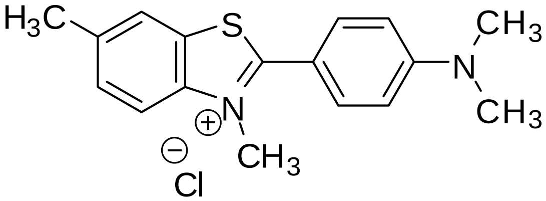

Figure 17. Thioflavin T

Circular Dichroism Spectroscopy

Circular dichroism (CD) is a powerful tool for investigating the structural properties of a protein, due to its sensitivity in monitoring secondary and tertiary structure. The difference in absorption is according to Lambert-Beer's law;

$$\Delta A = A_{left} - A_{right} = (\varepsilon_{left} - \varepsilon_{right}) * l * c = \Delta\varepsilon * l * c$$

where ΔA and $\Delta\varepsilon$ are defined as the differences in absorbance and molar absorptivity for left and right polarized light, l is the path length in cm and c is the molar concentration. Difference in absorption of left and right polarized light will occur if the molecule is placed in an asymmetrical environment or if the molecule contains or is covalently linked to a chiral center (Kelly et al., 2005).

The CD spectra of proteins are normally divided into two spectral regions; far UV (<240 nm) and near UV (240-320 nm) (Kelly et al., 2005).

Far-UV CD Spectra

The structure-specific CD bands that are seen in the far UV region originate from the regular arrangements of the polypeptide backbone into different types of secondary structure (α-helix, β-sheet, β-turns and random coil), see figure 18. The major chromophore in this region is the peptide bond that is covalently linked to the chiral α-carbon (Greenfield, 2004).

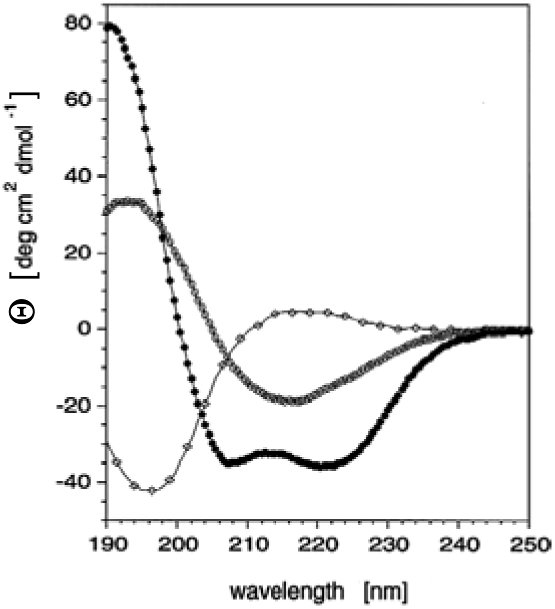

Figure 18. Far-UV CD spectra of different conformations of poly-L-lysine.
α-helical (filled circles), β-sheet (open circles) and random coil conformation (diamonds).
Redrawn from (Greenfield, 2004)

The Far-UV spectrum is used to estimate the amount of the different secondary structure elements in a protein, but it is known that both aromatic residues and disulphide bonds contributes to the Far-UV spectrum (Freskgard et al., 1994).

Near-UV CD Spectra

The near UV spectra are used to monitor the tertiary structure of a protein, and these spectra originate from the aromatic amino acids. When aromatic residues are located in asymmetric environments and interact with a unique surrounding tertiary structure they give rise to characteristic CD bands. This spectrum is very sensitive to changes in the tertiary structure, and can be used as a unique finger print of the native state for a protein (Freskgard et al., 1994; Kelly et al., 2005).

Transmission Electron Microscopy

Transmission electron microscopy (TEM) is a microscopy technique that uses a beam of electrons instead of light. The beam of high energy electrons is generated from a filament by a large accelerating voltage (80-400 kV). The beam is focused through electromagnetic condenser and objective lenses to focus the beam onto the sample. After the passage through the sample projector lenses expand the beam onto a phosphorescent screen and an imaging recording system such as a CCD camera.

There are different imaging methods in TEM and the one most used when investigating protein aggregates is bright field imaging mode. Here the contrast of the image is formed directly by absorption and scattering of the electrons by the sample. Regions in the sample with a higher atomic number will appear dark against a bright background. Biological samples consist mostly of carbon, which does not scatter or absorb electrons well and therefore such samples need to be stained. Uranyl acetate is used as a negative stain because of its high scattering of electrons and the capacity to adsorb well to biological matter. The staining also fixates the sample, helping it to withstand the harsh vacuum conditions required by TEM (Ruska, 1986).

Evaluation of protein stability

Protein unfolding as a function of denaturant can be detected by any method giving a detectable difference between the unfolded and the native protein. Figure 19 shows an example from the unfolding of HCA $\mathrm{II_{H107N}}$ by GuHCl, monitored by shift of wavelength maxima of the Trp fluorescence (λ_{max}) (Almstedt et al., 2008). Describing the reaction N ⇆ I ⇆ U where N is the native, I the intermediates and U the unfolded state.

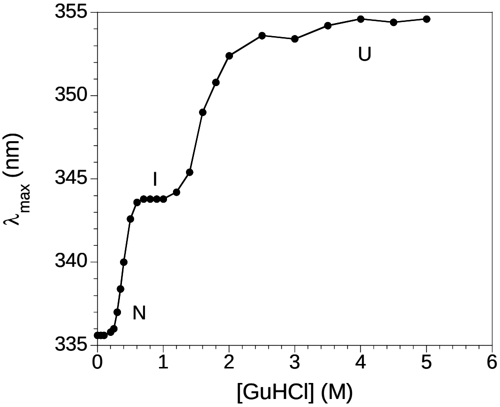

Figure 19. Stability of HCA $\mathrm{II_{H107N}}$ towards GuHCl denaturation. From (Almstedt et al., 2008)

Two requirements for this analysis to be applicable for quantification of stability are that the system must be reversible and that only two states of the protein exist in the transition region. If there are stable, populated intermediates between the native and unfolded states the free energy of unfolding is calculated for each transition separately (see figure 19).

The free energy of unfolding for the reaction is:

$$\Delta G = -RT\ln K$$

where ΔG are free energy of unfolding, R is the gas constant (1.987 cal/(K*mol)), T is the temperature in Kelvin and K represents the equilibrium constant, herein the ratio of unfolded/native protein at any specified denaturant concentration:

$$K = (y_N - y_{obs})/(y_{obs} - y_U)$$

y_N and y_U is λ_{max} are observables, here the for native and unfolded (or intermediate) protein, respectively, and y_{obs} is the observed λ_{max} at the given denaturant concentration.

ΔG is linearly dependent on the denaturant concentration (Santoro and Bolen, 1988), see figure 20, which can hereby be extrapolated to zero molar denaturant, according to the following equation:

$$\Delta G = \Delta G^{H2O} - m^*[\text{denaturant}]$$

where ΔG^{H2O} is the free energy for unfolding at zero molar denaturant.

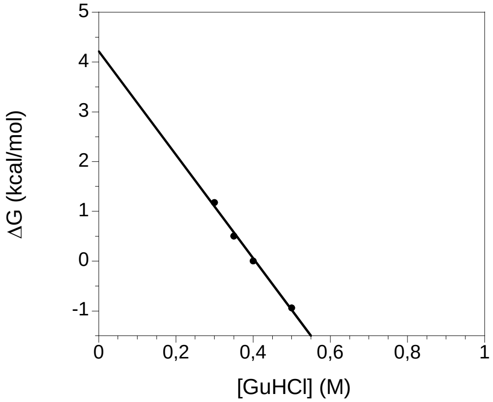

Figure 20. Dependence of free energy for unfolding of HCA II_{H107N} from the native state (N) to intermediate state (I) as a function of GuHCl.

If a protein variant is compared to the wild type protein the difference in ΔG^{H2O} ($\Delta\Delta G^{H2O}$) is an often used parameter, figure 21.

$$\Delta\Delta G^{H2O} = \Delta G^{H2O}{}_{(wt)} - \Delta G^{H2O}{}_{(mutant)}$$

Stabilization by ligand binding

A general consequence of ligand binding is that the protein is stabilized against unfolding and is less dynamic. Neither of these observations implies that the ligand has altered the conformation of the protein. Instead, they are simply a consequence of the ligand binding tightly to the fully folded conformation compared to the fully unfolded state and any distorted or partially unfolded forms that result from the flexibility of the structure. This can be illustrated by the following equation for the free energy of binding (ΔG_b):

$$\Delta G_b = -RT\ln ([A]/K_d)$$

where [A] is the concentration of free ligand and K_d is the dissociation constant, (Creighton, 1993). With a concentration equal of K_d half the protein molecules have bound ligand. If we were to assume the IC_{50} value to correspond to the dissociation constant we can theoretically estimate the binding energy of small molecule ligands to HCA II_{H107Y}. Two examples are shown below: binding of the strong inhibitor acetazolamide (10 μM) or the weaker inhibitor 4-amino-3,5-dichlorobenzenesulfonamide (10 μM) to HCA II_{H107Y} (0.8 μM) from paper III in this thesis:

$$\text{Free ligand } [A] = [\text{Ligand}] - [\text{HCA II}_{H107Y}] * \text{Fraction inhibited}$$

Acetazolamide

$$[A] = 10*10^{-6} - 0.8*10^{-6} * 1 = 9.2*10^{-6}\ M$$

$$IC_{50} \approx K_d = 2\ nM$$

$$\Delta G_b = -RT\ln(9.2*10^{-6} / 2*10^{-9}) = -\ 4.6\ kcal/mol$$

4-amino-3,5-dichlorobenzenesulfonamide

$$[A] = 10*10^{-6} - 0.8*10^{-6} * 0.72 = 9.4*10^{-6}\ M$$

$$IC_{50} \approx K_d = 1640\ nM$$

$$\Delta G_b = -RT\ln(9.4*10^{-6} / 1640*10^{-9}) = -\ 0.96\ kcal/mol$$

A ligand with strong inhibitory efficacy has in general a greater effect on the stability than one with weaker binding interaction, but this trend is not absolute; see paper III in this thesis.

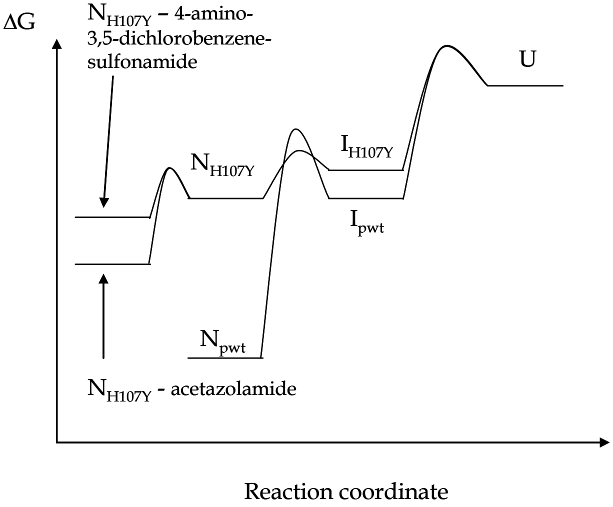
ΔG
N_{H107Y} – 4-amino-3,5-dichlorobenzene-sulfonamide
U
I_{H107Y}
N_{H107Y}
I_{pwt}
N_{pwt}
N_{H107Y} - acetazolamide
Reaction coordinate

Figure 21. Simplified energy diagram showing the reaction N ⇆ I ⇆ U for HCA II_{pwt} and HCA II_{H107Y} with and without bound inhibitors from paper III.

SUMMARY OF PAPERS

In this chapter a short summary of the papers included in this thesis will be presented. In the first three papers, mutants of the enzyme human carbonic anhydrase II have been used as a model system of a misfolding disease. The effects of the disease mutation has been investigated in the first two papers and in the third small molecular inhibitors and activators have been used to investigate their effectiveness to prevent the misfolding of the disease mutant.

In the fourth paper the amyloid fibrillation kinetics and aggregation of the human prion protein has been investigated during native like conditions *in vitro*.

Paper I and II

Many loss-of-function diseases are due to protein misfolding and one such disease is Carbonic Anhydrase II Deficiency Syndrome (CADS) (Shah et al., 2004; Sly et al., 1983). This disease is due to the absence of active HCA II and it is quite a rare disease, inherited in a recessive manner. The first identified mutation causing the disease was a His to Tyr substitution in position 107 (H107Y), and was first studied by Roth et al. in 1992 (Roth et al., 1992).

The HCA II$_{\mathrm{H107Y}}$ mutant has a native like active site

We were able to express this mutant in *E. coli* cells at 22˚C and purify it through aromatic sulfonamide affinity chromatography at 4˚C, which is a method that requires an intact active site. Also our results from enzyme activity assays showed that the mutant has an active site that is not altered in a way that terminates the enzymatic activity at 4 ˚C. Titration of the active site with the fluorescent probe 5-dimethylaminonaphtalene-1-sulfonamide (DNSA) showed an active site in all mutant molecules indicating a complete zinc ligand saturation of the mutant.

The native state of HCA II$_{H107Y}$ is extremely destabilized

The stability of HCA II$_{H107Y}$ towards chemical and thermal denaturation was monitored by enzyme activity, tryptophan fluorescence, near-UV CD and 1D-NMR.

The global unfolding of HCA II$_{H107Y}$ can be monitored by tryptophan fluorescence due to the even distribution of seven tryptophan residues. Denaturation of HCA II by GuHCl gives rise to a three-state unfolding profile, with an intermediate plateau populating the molten globule state. The midpoint concentration of denaturation and the Gibbs free energy of unfolding was calculated for each transition separately as described in p. 54-55 (Martensson et al., 1993; Santoro and Bolen, 1988). The native state stability of the mutant was decreased by 9.2 kcal/mol when denatured by GuHCl, see figure 22A and table 4, but the transition from the molten globule state to the unfolded state was not altered as much, indicating that the H107Y mutation affects the native state and that the intermediate state has very few specific tertiary interactions. When denaturated by temperature HCA II only unfolds to the molten globule state (Hammarstrom et al., 2001b; Persson et al., 1999) and the midpoint temperature of denaturation (T_m) was decreased from 61 ˚C to 22 ˚C for the mutant compared to the pseudo-wild type, giving rise to a ΔT_m of 39 ˚C, see figure 22B and table 4. When the temperature induced unfolding was monitored by the enzyme activity the T_m was also decreased by 39 ˚C, see figure 22C and table 4.

	$C_{m\,NI}$ (M) [a]	**$C_{m\,IU}$ (M)** [a]	**ΔG^{H2O}_{NI} (kcal/mol)** [a]	**ΔG^{H2O}_{IU} (kcal/mol)** [a]	**T_m (Flu.) (˚C)**	**T_m (CO_2) (˚C)**	**T_m (CD) (˚C)**
HCA II$_{pwt}$	1.05	1.62	9.6	6.5	61	55	>50
HCA II$_{H107Y}$	0.04	1.52	0.4	5.1	22	16	25

Table 4. Stability parameters. [a] Stabilities at 4 ˚C calculated from Trp fluorescence data. Midpoint concentration of denaturation (C_m) for native (N) to intermediate (I) states and for I to unfolded states (U). Gibbs free energies of unfolding were calculated for each transition and Gibbs free energy in water (ΔG^{H2O}) was obtained through linear extrapolation.

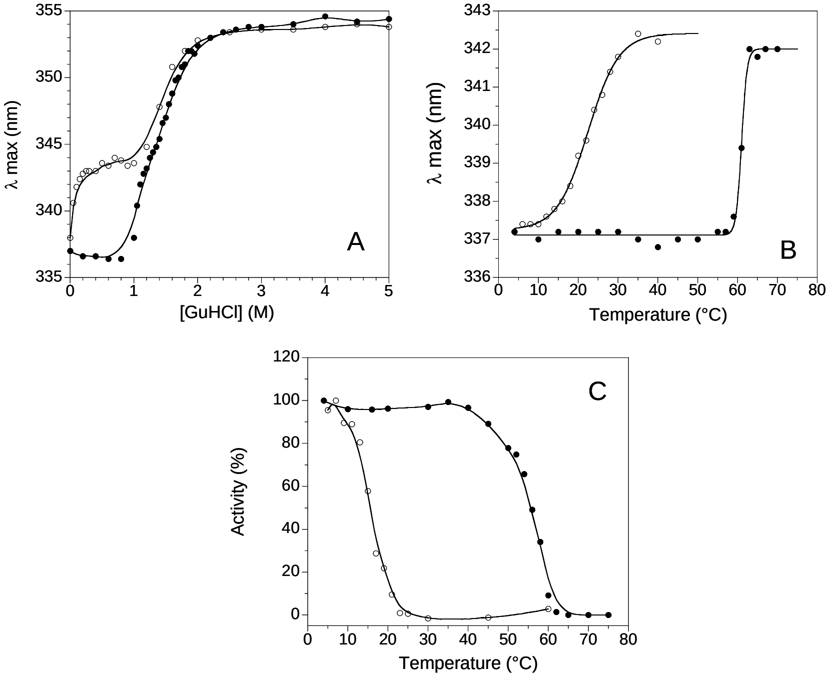

Figure 22. Stability of HCA II$_{pwt}$ (filled circles) and HCA II$_{H107Y}$ (open circles) towards chemical denaturation (A), and temperature denaturation (B and C). A) and B) shows the denaturation monitored by Trp fluorescence and C) CO$_2$ hydration activity assay.

The shape of the spectrum obtained for a protein by near-UV CD is a very sensitive tool for the tertiary structure of HCA II (Freskgard et al., 1994) and the spectrum of HCA II have the same features characteristic for native HCA II. Notably, the spectral bands have a lower ellipticity compared to HCA II$_{pwt}$, see figure 23. When the temperature denaturation was monitored by near-UV CD it showed a cooperative transition with a T$_m$ of 25 ˚C (figure 23, inset).

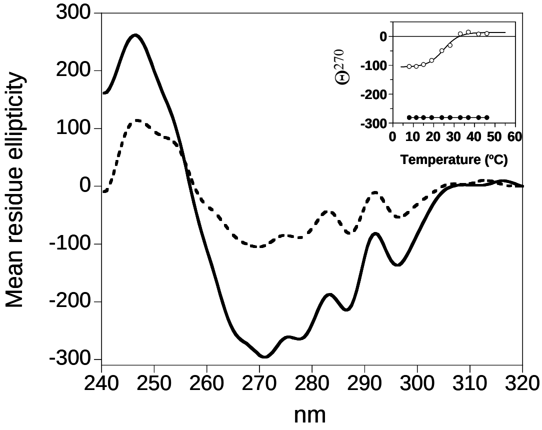

Figure 23. Near-UV CD spectra of HCA II$_{\mathrm{pwt}}$ (solid line) and HCA II$_{\mathrm{H107Y}}$ at 5˚C. The inset shows the mean residue ellipticity at 270 nm in the temperature range 8-50 ˚C for HCA II$_{\mathrm{H107Y}}$ (open circles) and HCA II$_{\mathrm{pwt}}$ (filled circles).

The 1-D NMR results showed that HCA II$_{\mathrm{H107Y}}$ undergoes a structural change between 22 ˚C and 25 ˚C.

HCA II$_{\mathrm{H107Y}}$ unfolds via an intermediate that is not aggregation prone

The denaturation of HCA II$_{\mathrm{H107Y}}$ is a stepwise process that starts with the disruption of the active site (T$_m$ = 16˚C), followed by solvent exposure of tryptophan residues (T$_m$ = 22˚C). Under physiological conditions (37 ˚C) this mutant is unable to fold into the native conformation. It will instead end up in a partially folded intermediate state. This intermediate state is observed by fluorescence from the hydrophobic probe 8-anilino-1-naphtalene sulphonic acid (ANS). When ANS is bound to a molten globule state its fluorescence maximum blue shifts from 520 nm to 480 nm (Andersson et al., 2001) and the quantum yield increases. During GuHCl denaturation HCA II$_{pwt}$ shows ANS binding with a peak at 1.2 M GuHCl and at this concentration the amount of ANS binding is the same for the mutant. However, the ANS binding of the mutant showed a plateau at relatively low concentrations of GuHCl prior the peak at 1.2 M GuHCl, see figure 24. This indicates that HCA II$_{H107Y}$ populates an early intermediate prior unfolding to the classical molten globule, described by us as the molten globule light state. The classical molten globule state has been proved to be aggregation prone (Hammarstrom et al., 2001b; Hammarstrom et al., 1999) due to the exposure of hydrophobic parts. We investigated the formation of aggregates by light scattering. The results showed that the aggregation temperature (T$_a$) of HCA II$_{pwt}$ is independent of protein concentration while the formation of HCA II$_{H107Y}$ aggregates is dependent on the concentration of protein, with a lower T$_a$ at higher protein concentrations.

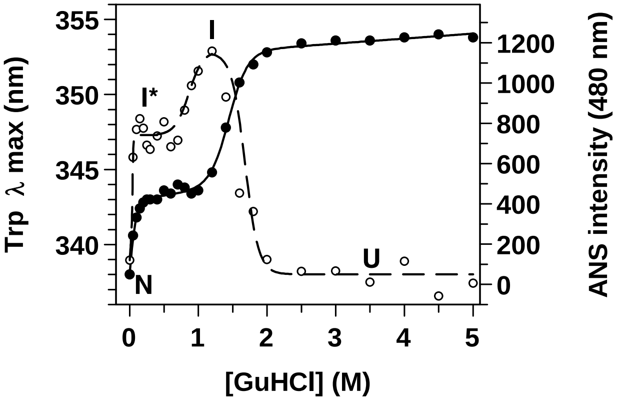

Figure 24. Comparison of Trp and ANS fluorescence of HCA II$_{H107Y}$ during GuHCl denaturation. Trp fluorescence in filled circles and ANS in open circles. The intermediate molten globule light is indicated with I* and the molten globule with I. Temperature 4°C.

Investigation of the H107 region in the HCA II structure

Molecular modeling of HCA II_{H107Y} indicated that the interactions between H107 and E117 are affected by the H107Y mutation, since it showed that two hydrogen bonds were lost by the mutation. It also indicated that new interactions are formed between Y107 and the surrounding structure including S29, which has previously been shown to be extremely important for the stability of HCA II (Martensson et al., 1992)

The positions of H107 and E117 are near the active site with distances of 7.6 Å and 10.2 Å respectively to the zinc atom. These amino acids are strictly conserved in active α-carbonic anhydrases, see figure 25, the only exceptions are found bacterial carbonic anhydrases in *Helicobacter pylori* (S117 instead of H107 and S127 instead of E117) and *Neisseria gonorrhea* (N99 instead of H107) (Almstedt et al., 2008; Chirica et al., 2001).

```
HCA_I       A------------------SPDWGYDD-KNGPEQWSKL---YP-IANGNNQSPVDIKTSE
HCA_II      -------------------SHHWGYGK-HNGPEHWHKD---FP-IAKGERQSPVDIDTHT
HCA_III     M------------------AKEWGYAS-HNGPDHWHEL---FP-NAKGENQSPIELHTKD
NGCA        -------------------HTHWGYTG-HDSPESWGNLSEEFRLCSTGKNQSPVNITETV
HPCA        MKKTFLIALALTASLVGAENTKWDYKNKENGPHRWDKLHKDFEVCKSGKSQSPINIEHYY

HCA_I       TKHDTSLKPISVSYNPATAKEIINVGHSFHVNFEDNQDRSVLKGGPFSDSYRLFQFHFHW
HCA_II      AKYDPSLKPLSVSYDQATSLRILNNGHAFNVEFDDSQDKAVLKGGPLDGTYRLIQFHFHW
HCA_III     IRHDPSLQPWSVSYDGGSAKTILNNGHTCNVVFDDTYDRSMLRGGPLPGPYRLRQFHLHW
NGCA        SG---KLPAIKVNYKPS-MVDVENNGHTIQVNYPEGGNTLTVNGR----TYTLKQFHFHV
HPCA        HTQDK--ADLQFKYAASKPKAVFFTHHTLKASFEPTN-HINYRGH----DYVLDNVHFHA

                     ↓         ↓
HCA_I       GSTNEHGSEHTVDGVKYSAELHVAHWNSAKYSSLAEAASKADGLAVIGVLMKVGEANPKL
HCA_II      GSLDGQGSEHTVDKKKYAAELHLVHWNT-KYGDFGKAVQQPDGLAVLGIFLKVGSAKPGL
HCA_III     GSSDDHGSEHTVDGVKYAAELHLVHWNP-KYNTFKEALKQRDGIAVIGIFLKIGHENGEF
NGCA        P------SENQIKGRTFPMEAHFVHLDE-N-----------KQPLVLAVLYEAGKTNGRL
HPCA        P------MEFLINNKTRPLSAHFVHKDA-K-----------GRLLVLAIGFEEGKENPNL

HCA_I       QKVLDALQAIKTKGKRAPFTNFDPSTLLPSSLDFWTYPGSLTHPPLYESVTWIICKESIS
HCA_II      QKVVDVLDSIKTKGKSADFTNFDPRGLLPESLDYWTYPGSLTTPPLLECVTWIVLKEPIS
HCA_III     QIFLDALDKIKTKGKEAPFTKFDPSSLFPASRDYWTYQGSFTTPPCEECIVWLLLKEPMT
NGCA        SSIWNVMP--MTAGKVKLNQPFDASTLLPKRLKYYRFAGSLTTPPCTEGVSWLVLKTYDH
HPCA        DPILEGIQ------KKQNFKEVALDAFLPKSINYYHLTA--LSPLLLAQRGWHG------

HCA_I       VSSEQLAQFRSLLSNVEGDNAVPMQHNNRPTQPLKGRTVRAS-F
HCA_II      VSSEQVLKFRKLNFNGEGEPEELMVDNWRPAQPLKNRQIKASFK
HCA_III     VSSDQMAKLRSLLSSAENEPPVPLVSNWRPPQPINNRVVRASFK
NGCA        IDQAQAEKFTRAVG----------SENNRPVQPLNARVV---IE
HPCA        -------------------------------------------L
```

Figure 25. Amino acid sequences of human carbonic anhydrase I-III, *N. gonorrhea* carbonic anhydrase and *H. pylori* carbonic anhydrase.

The conserved residues H107 and E117 in HCA II are shown with arrows.

The modeling indications, invariance in the positions involved and the extreme destabilization of the disease mutant encouraged us to investigate these positions more thoroughly with a mutational study.

Five single mutants (H107Y, H107F, H107A, H107N and E117A) and two double mutants (H107A/E117A and H107N/E117A) were generated with the pseudo-wild type as background. The mutations H107A and E117A were made to remove the side chains and thereby the hydrogen bonds between residues H107 and E117. H107F was constructed to remove the ability to form hydrogen bonds while retaining the sterical properties of the tyrosine and H107N was designed with respect to the carbonic anhydrase from *N. gonorrhea*. The double mutants were made to probe the interaction energy between H107 and E117 using a double mutant cycle.

The mutants were characterized using temperature denaturation (monitored by Trp fluorescence and enzyme activity), chemical denaturation (monitored by Trp fluorescence) and ANS fluorescence. The stability data are summarized in table 5. The double mutants were already in the molten globule state at 4 ˚C, which makes it impossible to calculate midpoints of denaturation for the first transition. This proved to be possible by use of small molecule stabilization for H107N/E117A, see below. Notably, all mutants in position 107 and the mutant in position 117 were very destabilizing, demonstrating the stabilizing importance of these highly conserved residues in HCA II.

	$C_{m\,NI}$ (M) [a]	$C_{m\,IU}$ (M) [a]	ΔG^{H2O}_{NI} (kcal/mol) [a]	T_m (Flu.) (˚C)	T_m (CO_2) (˚C)	% molten globule of pwt
HCA II$_{pwt}$	1.05	1.62	9.6	61	55	100
H107Y	0.04	1.52	0.4	22	16	175
H107A	0.14	1.66	1.3	32	27	82
H107F	0.08	1.66	1.0	24	21	110
H107N	0.41	1.66	4.2	40	40	103
E117A	0.56	1.53	4.9	34	33	133
H107A/E117A	ND	ND	-3.4[b]	<<4	ND	ND
H107N/E117A	-	1.70	-0.1[b]	<4	ND	68

Table 5. Stability parameters. [a] Stabilities calculated from Trp fluorescence data.
[b] Calculated value, see main text for details.

All single mutants showed native-like near-UV CD spectral features at 4 ˚C but with decreased amplitudes compared to the pseudo wild-type.

ANS was used to determine the amount of molten globule formed during denaturation by GuHCl. The amount of ANS bound to the molten globule was determined by integrating the total ANS fluorescence in the 0-2 M interval of GuHCl where all mutants and HCA II$_{pwt}$ had a populated molten globule, data are shown in table 5. The high binding of ANS to H107Y, H107F and E117A indicates that these mutants populate both the molten globule light state and the molten globule state. H107N and HCA II$_{pwt}$ are probably only populating the molten globule state and H107N/E117A is probably shifted towards a more unfolded state incapable of ANS binding. The reason why H107A shows decreased ANS binding is not known.

The destabilization of HCA II$_{H107Y}$ is due to long distance interactions

Aromatic sulfonamide affinity chromatography purification of the double mutant H107N/E117A was successful, showing that the mutant can fold to a native structure in the presence of an inhibitor. The inhibitor appeared to function as a chemical chaperone and therefore we used the small molecule inhibitor acetazolamide to induce folding of the mutant. To quantify the stabilizing effects all mutants were incubated with acetazolamide prior to denaturation by GuHCl and the mutants were stabilized by 0.8-3.2 kcal/mol. Using the data from the single mutants we could calculate the ΔG^{H2O} value for the double mutant without inhibitor bound. The calculated stability for the double mutant was only 0.1 kcal/mol, likely explaining why the H107N/E117A mutant is unfolded even at 0 M GuHCl at 4 ˚C.

From a double mutant cycle we could calculate the interaction energy (ΔG_{int}) between H107 and E117:

$$\Delta G_{int} = \Delta\Delta G_{NI}{}^{pwt\text{-}H107N} + \Delta\Delta G_{NI}{}^{pwt\text{-}E117A} - \Delta\Delta G_{NI}{}^{pwt\text{-}H017N/E117A} =$$

$$5.4 + 4.7 - (9.6 - 0.1) = 0.6 \text{ kcal/mol}$$

This method has previously been used to show the importance of salt bridges and electrostatic interactions in the folding and stability of several proteins (Horovitz et al., 1990; Luisi et al., 2003; Makhatadze et al., 2003; Tissot et al., 1996). The interaction energy between H107 and E117 was almost negligible and the destabilizing effects of H107Y and E117A were essentially additive. This independence of stabilization between these two interacting residues is surprising and shows that the direct interaction is not responsible for the destabilization, but rather due to the disturbances in the H-bond network surrounding the active site.

Paper III

The findings that the binding of a small-molecular inhibitor (acetazolamide) could stabilize the mutants by 0.8-3.2 kcal/mol in paper I and II encouraged us to investigate if the use of other carbonic anhydrase inhibitors (CAIs) could prevent misfolding of HCA II_{H107Y}. We selected 9 inhibitors (see table 6) to get a wide spectrum of poor to very strong binders to address whether the best binders also were superior in preventing misfolding.

The different sulfonamide inhibitors were tested for their inhibition efficiency of HCA II_{pwt} and HCA II_{H107Y}. We used the CO_2 hydration activity assay (Rickli et al., 1964) and obtained the inhibitory concentration at 50 % enzyme activity (IC_{50}), see table 6.

Inhib.#	Structure	Name	IC_{50} (H107Y) nM	IC_{50} (HCA II) nM
1	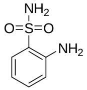	2-Amino-benzenesulfonamide	248	235
2	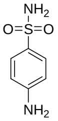	4-Amino-benzenesulfonamide	60	43
3	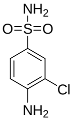	4-Amino-3-chloro-benzenesulfonamide	70	65
4	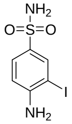	4-Amino-3-iodo-benzenesulfonamide	145	80
5	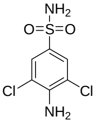	4-Amino-3,5-dichloro-benzenesulfonamide	1640	553
6	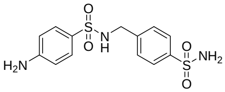	4-Amino-N-(4-sulfamoylbenzyl)-benzenesulfonamide	13	6
7	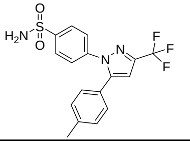	4-(5-p-Tolyl-3-trifluoromethyl-pyrazol-1-yl)-benzenesulfonamide	96	145
8	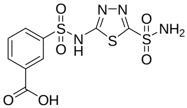	3-(5-sulfamoyl-1,3,4-thiadiazol-2-ylsulfamoyl)-benzoic acid	31	16
9	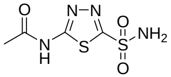	2-acetylamido-1,3,4-thiadiazole-5-sulfonamide	2	8

Table 6. IC_{50} values of compounds 1-9 on HCA II_{pwt} and HCA II_{H107Y}

The stabilization capacities of the different inhibitors were measured by Trp fluorescence towards both thermal denaturation and denaturation by GuHCl at 4˚C. All unfolding curves in presence of inhibitors showed the same unfolding profiles, see figure 26 A-C, but with higher midpoints of thermal denaturation (T_m) and midpoint concentrations of GuHCl (C_m) compared to the unliganded mutant, see table 7.

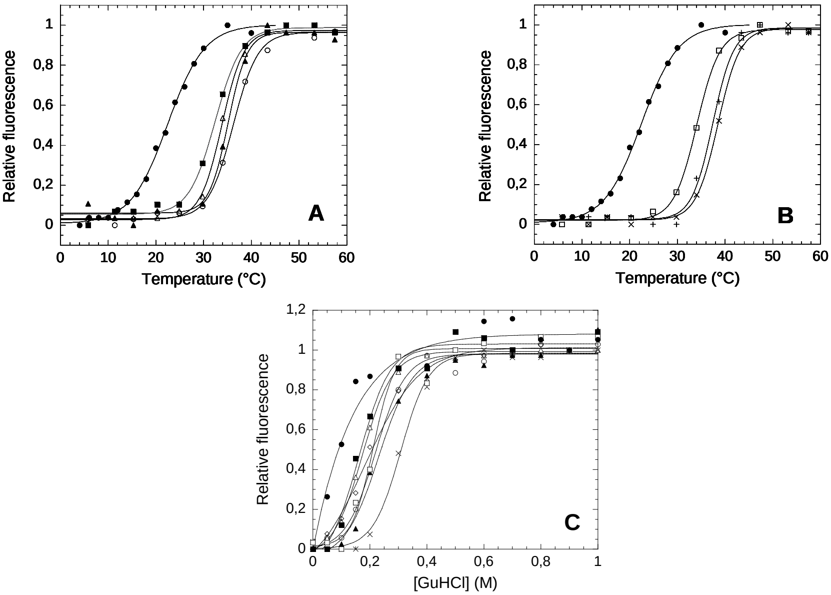

Figure 26 A and B. Stability of HCA $\mathrm{II}_{\mathrm{H107Y}}$ towards thermal denaturation. The enzyme concentration was 0.8 µM in 100 mM sodium borate, pH 7.5, and the final concentration of the inhibitors was 10 µM. **Figure 26 C.** Stability of HCA $\mathrm{II}_{\mathrm{H107Y}}$ towards denaturation by GuHCl at 4˚C. The figure shows the transition from native state to the intermediate state. The enzyme concentration was 0.8 µM in 100 mM sodium borate, pH 7.5, and the final concentration of the inhibitors was 10 µM. (●) no inhibitor; (○) inhibitor 2; (▲) inhibitor 3; (Δ) inhibitor 4; (■) inhibitor 5; (x) inhibitor 6; (◊) inhibitor 7; (□) inhibitor 8.

Inhibitor	**C_m N→I (M)**	**ΔC_m N→I (M)**	**ΔG_{H2O} N→I (kcal/mol)**	**$\Delta\Delta G_{H2O}$ N→I (kcal/mol)**	**T_m 1:1 (˚C)**	**ΔT_m 1:1 (˚C)**	**T_m 12:1 (˚C)**	**ΔT_m 12:1 (˚C)**
-	0.09	-	1.1	-	22	-	22	-
2	0.24	0.15	2.8	-1.7	31	9	36	14
3	0.22	0.13	2.2	-1.1	30	8	35	13
4	0.18	0.09	2.1	-1.0	30	8	34	12
5	0.19	0.10	1.9	-0.8	23	1	32	10
6	0.32	0.23	3.7	-2.6	29	7	38	16
7	0.20	0.11	1.6	-0.5	29	7	37	15
8	0.21	0.12	2.3	-1.2	29	7	34	12
9	0.28*	0.24*	3.4*	-3.0*	33	11	34*	16*

Table 7. Stability data of unfolding of the native state of HCA II$_{H107Y}$ in the presence of compounds 2-9.
* The data for inhibitor 9 (acetazolamide) are from our previously study (Almstedt et al., 2004)

Unfortunately the stability in the presence of inhibitor **1** could not be measured due to intrinsic fluorescence of **1** when bound to HCA II. Inhibitors **2-5** are simple para-amino substituted benzo-sulfonamides and the introduction of one or two halo-substituents in meta position lowers their stabilizing effects. For these inhibitors the decrease in stabilizing effect was reflected in the IC$_{50}$ values, with decrease in parallel to the stabilizing effects.

The more complex inhibitors (**6-9**) showed a more complex correlation pattern between the stabilizing effects and inhibition potency *i.e.* inhibitor **7** has a higher IC$_{50}$ value (lower inhibition effect) than inhibitor **8** and shows a higher potency than **8** against thermal denaturation but a significantly lower stabilizing effect towards chemical denaturation, see figure 27, table 6 and table 7.

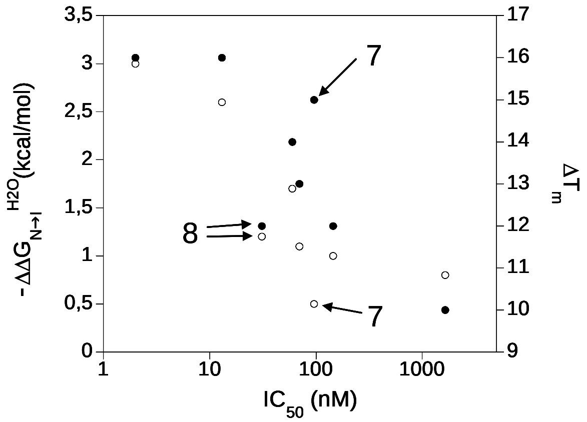

Figure 27. Correlation between the stabilization effects of GuHCl determined stability (4˚C) and the thermal stability (T_m) of HCA II_{H107Y} in the first unfolding transition versus the IC_{50} values for the different inhibitors. (○) $-\Delta\Delta G_{N\rightarrow I}^{H2O}$ (kcal/mol); (●) ΔT_m (˚C).

In the perfect scenario the inhibitor should stabilize the protein so the T_m is above 37 ˚C but at the same time have a high enough IC_{50} value to allow a fraction of enzyme molecules to be free of the inhibitor and able to perform catalysis. In our case the disease mutant is so extremely destabilized only the most potent inhibitors could stabilize the protein so that half of the protein molecules were in the native form at 37 ˚C, but at the high concentration this demanded all activity was lost.

There are several reported activators of HCA II known (CAAs)(Temperini et al., 2005; Temperini et al., 2006a, b) and we wanted to investigate if they could have any effect on the activity and stability of the disease mutant. We chose the activators L-His, L-Phe and D-Phe for this study. Activators applied at high concentrations (750-fold molar excess) increased the CO_2 hydration activity for HCA II_{H107Y} to 162 % for L-His, but no increase was observed for L-Phe or D-Phe.

The thermal stability was measured with the activators present at 12-fold molar excess, but no stabilizing effect was observed for any of the activators, see inset in figure 28. We thereafter investigated if the binding of the activators could slow down the kinetics of thermal unfolding. At 37 °C the enzyme activity was lost within a few minutes for the unliganded HCA II_{H107Y}, see figure 27. There were no alteration in the decay rate when the activators were present even in a 750-fold molecular excess. The inefficiency of the CAAs compared to the CAIs indicates that shifting the equilibrium towards the native state necessitates a firm anchoring site in HCA II, a characteristic lacking for the activator binding site, at the outer rim of the active site (Temperini et al., 2006b).

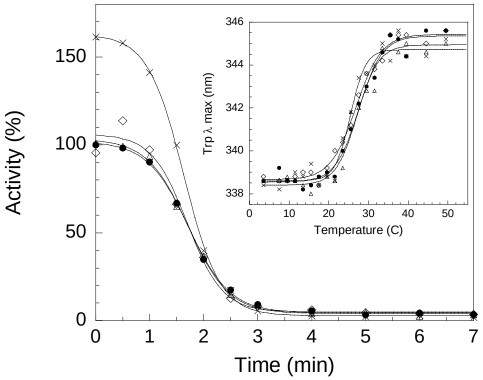

Figure 28: Thermal stability kinetics for HCA II_{H107Y} with different activators at 750-fold molar excess at pH 8.0. The inset shows temperature denaturation curves for HCA II_{H107Y} with different activators at 12-fold molar excess. (●) no activator; (x) L-His; (◊) L-Phe; (Δ) D-Phe.

Paper IV

Prion diseases can be sporadic, inherited and infectious diseases. The initial finding that scrapie associated infections prions formed amyloid-like structures was shown 25 years ago by Prusiner and Glenner (Prusiner et al., 1983). Following the discovery that prions are composed of a normally neurotropic protein, PrP^C, conformational conversion of PrP^C into a misfolded state, PrP^{Sc}, that is aggregation prone and forms amyloid fibrils has gained acceptance as the causative agent in all prion diseases (Aguzzi, 2008). Hence aggregation and amyloidogenesis of PrP is strongly correlated with prion disease and is an intense research field (Aguzzi, 2008). Amyloid fibrillation and oligomer formation of PrP in *in vitro* studies have so far been performed under conditions where mild to harsh conditions of denaturants of various sorts have been included. In this work we show the unusual behavior of recombinant human prion protein during protein aggregation and fibrillation when performed under non-denaturing conditions close to physiological.

Formation of amyloid fibrils of recombinant human PrP under physiological conditions

Three HuPrP variants: ${}^{His}HuPrP_{90\text{-}231}$, $HuPrP_{90\text{-}231}$ and ${}^{His}HuPrP_{121\text{-}231}$, (${}^{His}HuPrP_{121\text{-}231}$, human prion protein sequence 121-231 with an N-terminal hexa histidine tag; ${}^{His}HuPrP_{90\text{-}231}$, human prion protein sequence 90-231 with an N-terminal hexa histidine tag; $HuPrP_{90\text{-}231}$, human prion protein sequence 90-231) were purified as native monomers using size exclusion chromatography with a nearly physiological buffer (buffer F: 100 mM NaCl, 50 mM KCl, 50 mM phosphate, pH 7.4) at room temperature.

To induce amyloid fibril formation we used intense shaking (350 rpm) of the folded protein in partially filled, sealed plastic tubes in buffer F at 37 ˚C. Under these gentle conditions we could induce irreversible conversion of native recombinant HuPrP variants into aggregates composed of amyloid fibrils within hours. Formed aggregates were positive using Thioflavin T (ThT) fluorescence and showed Congo red birefringence under polarized light. Fibrillar morphology was verified by transmission electron microscopy. These methods show that the initial native largely helical native recombinant HuPrP variants had misfolded into the aggregated state of cross-β-sheet structure of amyloid.

Amyloid fibrillation kinetics followed by Thioflavin T

The rate of amyloid fibril formation was analyzed using Thioflavin T, ThT fluorescence. A large number of identical samples were subjected to fibrillation conditions in buffer F under intense shaking (350 rpm) at 37 °C (as above) and aliquots were taken at different time points to be assayed for ThT fluorescence. The amyloid fibrillation kinetics followed a trajectory with a lag phase, a growth phase and an equilibrium phase. The longest lag-phase in the spontaneous fibrillation kinetics was obtained for $^{His}HuPrP_{90\text{-}231}$, hence this variant was selected for seeding experiments. Samples were run using preformed fibrils as seeds at two different concentrations (1% and 5% of the total amount of protein). As expected the lag phase was shortened for the seeded reactions and the final ThT signal was higher, indicating a more efficient conversion into the amyloid fibrillar state, see figure 29.

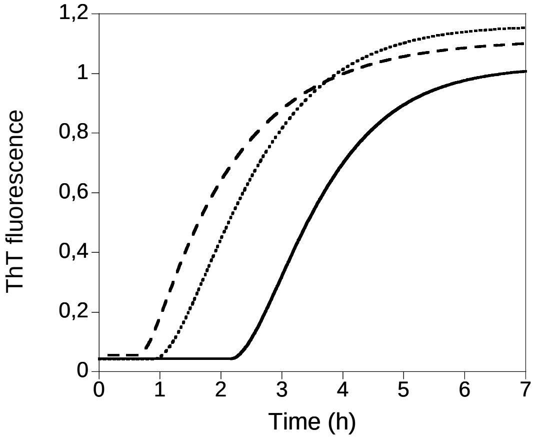

Figure 29. Average fibrillation kinetics curves for ^{His}HuPrP$_{90\text{-}231}$ (solid line), with 1% seed (dotted line) and with 5% seed (dashed line)

Amyloid fibrils are formed after initial aggregation

During sampling of the fibrillation reaction we noted that samples were turbid already after a few minutes of fibrillation conditions, long before any ThT fluorescence appeared. To quantify the aggregation rate we subjected identical samples of ^{His}HuPrP$_{90\text{-}231}$ to turbidity measurements. Comparing the trace of turbidity with the onset of ThT fluorescence revealed dramatically different kinetics, figure 30b.

At different time points aliquots were withdrawn and analyzed by transmission electron microscopy to assess the morphology of the formed ^{His}HuPrP$_{90\text{-}231}$ aggregates. From the micrographs it was evident that early formed aggregates up to 2 h was composed of heavily clustered material which over time (>2 h) transformed into fibrillar material, figure 30a.

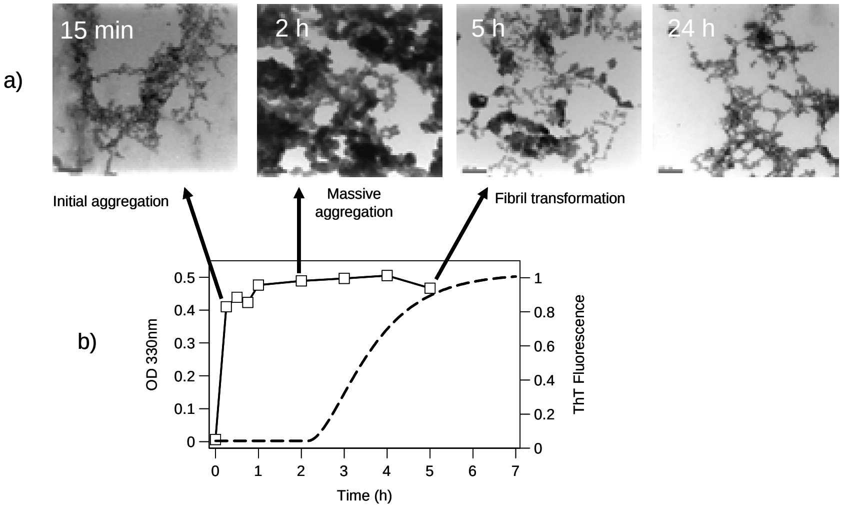

Figure 30. a) Morphology of ^{His}HuPrP$_{90\text{-}231}$ aggregates during fibrillation. Transmission electron microscopy images of negatively stained aggregates at different time points taken at 200000 fold magnification, showing the conversion of disordered aggregates towards fibrils over time. Scale bar represent 100 nm. b) Kinetic traces of turbidity at 330 nm (open squares) and the fitted ThT fluorescence (dashed trace), run under identical conditions.

Interestingly, lowering the protein concentration to half does not affect the lag phase but increased the rate of fibril growth. Taken together this suggests that the initial aggregation can function as a kinetic trap that decelerates initial nucleation into a fibrillation competent nucleus, but without aggregation there was no onset of amyloid fibrillation. The morphologically disordered aggregates can undergo a sol-gel conversion into rigid well organized amyloid fibrils, resulting in a distinct phase transition. This type of prion protein conversion could be important for understanding the molecular mechanism of PrP^{C} to PrP^{Sc} conversion in prion diseases.

CONCLUSIONS

From the studies in this thesis it can be concluded that:

- The disease causing mutant of HCA II investigated in this thesis (HCA II_{H107Y}) is extremely destabilized and has no enzymatic activity under physiological conditions. It unfolds via ensembles of intermediates that are not as aggregation prone as the classic molten globule, *i.e.* do not expose as many hydrophobic regions to the solution.

- To understand the consequences of mutations causing protein misfolding, one needs to take into account not only the lost native residue contacts, but also possible destabilizing interactions from the introduced residue. Furthermore, compensatory interactions can partially restore lost stabilizing contacts, and the network of interactions in a large folded protein is rarely binary.

- Binding of a small ligand can shift the equilibrium between the native state and intermediate states towards the native state and thereby induce folding. This strategy has the potential to be fruitful for "pharmacological chaperoning" of misfolding diseases.

- Amyloid fibril formation of HuPrP can be induced by intense agitation under otherwise physiological conditions. Agitation confers continuous exposure to the air-water interface known to be severely destabilizing conditions for proteins, suggesting that transient exposure to denaturing conditions can irreversible nucleate HuPrP aggregation.

- Amyloid fibrils of $^{His}HuPrP_{90\text{-}231}$ are formed from disordered aggregates in a conversion process that occur in a sol-gel phase, suggesting that amyloid fibrillation and apparently amorphous aggregation are not fundamentally different processes.

- The lag phase of $^{His}HuPrP_{90\text{-}231}$ appeared to be due to nucleation as seeding with preformed fibrils significantly shortened the lag phase. Also lowering the protein concentration to half do not affect the lag phase but increased the rate of fibril growth. Taken together this suggests that the initial aggregation can function as a kinetic trap that decelerates initial nucleation into a fibrillation competent nucleus, but without aggregation there was no onset of amyloid fibrillation.

ACKNOWLEDGEMENTS

I det här viktiga (och troligtvis mest lästa) kapitel vill jag tacka de människor som på ett eller annat sätt har hjälpt mig genom åren som doktorand.
Om inte ni hade stått bakom mig hade den här boken aldrig blivit skriven.

Tack!

Per Hammarström, min handledare och idékläckare. Jag är helt övertygad om att jag inte kunde haft mer tur med att hitta en bättre handledare. Med din enorma kunskap och entusiasm som lätt smittar av sig har du gjort mitt arbete här både roligt och lärorikt!

Uno och Lasse, tack för all hjälp med karboanhydras projekten!

Peter, det är alltid roligt att diskutera med någon som kan så mycket!

Therés Rafstedt, min första och sista exjobbare. Utan din eviga energi hade inte inhibitor-peket blivit vad det blev!

Sofie, många skratt och tårar har det blivit genom åren. Dina råd har hjälpt mig på alla sätt!

Patricia, sedan du flyttade in på kontoret har det bara varit roligt att gå till jobbet! Tack för att du orkar dela med dig av din positiva energi!

Veronica och Anngelica; bra vänner, bra kollegor och bra resesällskap. Kom ihåg att livet måste vara lite ”Palan, palan” ibland!

Mina gruppmedlemmar: **Ina, Therése, Minna, Satish, Daniel S och Karin**. Tack för alla ideér och förslag som ni har gett mig under våra gruppmöten och trevliga kafferaster!

Alla vänner och kollegor runt runda bordet; **Cissi, Maria, Daniel K, Daniel N, Andreas, Elna, Sara, Fredrik, Scarlett och Linda**. Utan er hade inte en lunchlåda varit dagens höjdpunkt!

Utan de riktiga kemisterna skulle kemifesterna vara torra, tråkiga och antagligen för få... Speciellt tack till **Alma** för all hjälp med trilskandes molekyler och trevligt träningssällskap!

Martin K och Karin C, ni var de bästa labkompisar man kan tänka sig och ni visade mig att även doktorander är vanliga människor!

Amanda, Laila och Louise, tack för alla trevliga samtal om allt mellan himmel och jord!

Lotta och Klara, ni har varit en fast punkt att falla tillbaka på när det känts jobbigt!

Anna, tack för ditt engagemang, stöd och för att du hjälpt mig att se det som egentligen är viktigt!

Min familj, som alltid har funnits där när jag behövt det som mest!

REFERENCES

Aguzzi, A. (2008). Staining, straining and restraining prions. Nature neuroscience *11*, 1239-1240.

Almstedt, K., Lundqvist, M., Carlsson, J., Karlsson, M., Persson, B., Jonsson, B.H., Carlsson, U., and Hammarstrom, P. (2004). Unfolding a folding disease: folding, misfolding and aggregation of the marble brain syndrome-associated mutant H107Y of human carbonic anhydrase II. Journal of molecular biology *342*, 619-633.

Almstedt, K., Martensson, L.G., Carlsson, U., and Hammarstrom, P. (2008). Thermodynamic interrogation of a folding disease. Mutant mapping of position 107 in human carbonic anhydrase II linked to marble brain disease. Biochemistry *47*, 1288-1298.

Andersson, D., Hammarstrom, P., and Carlsson, U. (2001). Cofactor-induced refolding: refolding of molten globule carbonic anhydrase induced by Zn(II) and Co(II). Biochemistry *40*, 2653-2661.

Anfinsen, C.B. (1973). Principles that govern the folding of protein chains. Science (New York, NY *181*, 223-230.

Baldwin, R.L. (1994). Protein folding. Matching speed and stability. Nature *369*, 183-184.

Baldwin, R.L. (1995). The nature of protein folding pathways: the classical versus the new view. Journal of biomolecular NMR *5*, 103-109.

Bayliss, N., and McRae, E. (1954). Solvent Effects in Organic Spectra: Dipole Forces and the Franck–Condon Principle. The Journal of Physical Chemistry *58*, 1002-1006.

Bornscheuer, U.T., and Buchholz, K. (2005). Highlights in Biocatalysis - Historical Landmarks and Current Trends. Engineering in Life Sciences *5*, 309-323.

Brown, D.R., Qin, K., Herms, J.W., Madlung, A., Manson, J., Strome, R., Fraser, P.E., Kruck, T., von Bohlen, A., Schulz-Schaeffer, W., *et al.* (1997). The cellular prion protein binds copper in vivo. Nature *390*, 684-687.

Brown, P., Gibbs, C.J., Jr., Rodgers-Johnson, P., Asher, D.M., Sulima, M.P., Bacote, A., Goldfarb, L.G., and Gajdusek, D.C. (1994). Human spongiform encephalopathy: the National Institutes of Health series of 300 cases of experimentally transmitted disease. Annals of neurology *35*, 513-529.

Bryngelson, J.D., Onuchic, J.N., Socci, N.D., and Wolynes, P.G. (1995). Funnels, pathways, and the energy landscape of protein folding: a synthesis. Proteins *21*, 167-195.

Bucciantini, M., Giannoni, E., Chiti, F., Baroni, F., Formigli, L., Zurdo, J., Taddei, N., Ramponi, G., Dobson, C.M., and Stefani, M. (2002). Inherent toxicity of aggregates implies a common mechanism for protein misfolding diseases. Nature *416*, 507-511.

Bueler, H., Fischer, M., Lang, Y., Bluethmann, H., Lipp, H.P., DeArmond, S.J., Prusiner, S.B., Aguet, M., and Weissmann, C. (1992). Normal development and behaviour of mice lacking the neuronal cell-surface PrP protein. Nature *356*, 577-582.

Camacho, C.J., and Thirumalai, D. (1993). Kinetics and thermodynamics of folding in model proteins. Proceedings of the National Academy of Sciences of the United States of America *90*, 6369-6372.

Chan, H.S., and Dill, K.A. (1994). Transition states and folding dynamics of proteins and heteropolymers. Journal of Chemical Physics *100*, 9238-9257.

Chan, H.S., and Dill, K.A. (1996). Comparing folding codes for proteins and polymers. Proteins *24*, 335-344.

Chang, T.-L., and Cheung, H.C. (1990). A model for molecules with twisted intramolecular charge transfer characteristics: solvent polarity effect on the nonradiative rates of dyes in a series of water-ethanol mixed solvents. Chemical Physics Letters *173*, 343-348.

Chirica, L.C., Elleby, B., and Lindskog, S. (2001). Cloning, expression and some properties of alpha-carbonic anhydrase from Helicobacter pylori. Biochimica et biophysica acta *1544*, 55-63.

Chiti, F., Webster, P., Taddei, N., Clark, A., Stefani, M., Ramponi, G., and Dobson, C.M. (1999). Designing conditions for in vitro formation of amyloid protofilaments and fibrils. Proceedings of the National Academy of Sciences of the United States of America *96*, 3590-3594.

Collinge, J. (1999). Variant Creutzfeldt-Jakob disease. Lancet *354*, 317-323.

Collinge, J. (2001). Prion diseases of humans and animals: their causes and molecular basis. Annual review of neuroscience *24*, 519-550.

Collins, S.J., Lawson, V.A., and Masters, C.L. (2004a). Transmissible spongiform encephalopathies. Lancet *363*, 51-61.

Collins, S.R., Douglass, A., Vale, R.D., and Weissman, J.S. (2004b). Mechanism of prion propagation: amyloid growth occurs by monomer addition. PLoS biology *2*, e321.

Conway, K.A., Lee, S.J., Rochet, J.C., Ding, T.T., Williamson, R.E., and Lansbury, P.T., Jr. (2000). Acceleration of oligomerization, not fibrillization, is a shared property of both alpha-synuclein mutations linked to early-onset Parkinson's disease: implications for pathogenesis and therapy. Proceedings of the National Academy of Sciences of the United States of America *97*, 571-576.

Creighton, T.E. (1990). Protein folding. The Biochemical journal *270*, 1-16.

Creighton, T.E. (1993). Proteins. Structures and Molecular Properties (New York, W.H. Freeman and Company).

Das, K., Sarkar, N., and Nath, D. (1992). Nonradiative pathways of aniline-naphtalene sulphonates: twisted intramolecular charge transferversus intersystem crossing. Spectrochimica Acta *48A*, 1701-1705.

Dill, K.A., and Chan, H.S. (1997). From Levinthal to pathways to funnels. Nature structural biology *4*, 10-19.

Dinner, A.R., Sali, A., Smith, L.J., Dobson, C.M., and Karplus, M. (2000). Understanding protein folding via free-energy surfaces from theory and experiment. Trends in biochemical sciences *25*, 331-339.

Dobson, C.M. (1999). Protein misfolding, evolution and disease. Trends in biochemical sciences *24*, 329-332.

Dobson, C.M. (2003). Protein folding and misfolding. Nature *426*, 884-890.

Dobson, C.M., Sali, A., and Karplus, M. (1998). Protein Folding: A perspective from theory and experiment. Angewandte Chemie International Edition *37*, 868-893.

Ecroyd, H., and Carver, J.A. (2008). Unraveling the mysteries of protein folding and misfolding. IUBMB life *60*, 769-774.

Fink, A.L. (1998). Protein aggregation: folding aggregates, inclusion bodies and amyloid. Folding & design *3*, R9-23.

Freskgard, P.O., Carlsson, U., Martensson, L.G., and Jonsson, B.H. (1991). Folding around the C-terminus of human carbonic anhydrase II. Kinetic characterization by use of a chemically reactive SH-group introduced by protein engineering. FEBS letters *289*, 117-122.

Freskgard, P.O., Martensson, L.G., Jonasson, P., Jonsson, B.H., and Carlsson, U. (1994). Assignment of the contribution of the tryptophan residues to the circular dichroism spectrum of human carbonic anhydrase II. Biochemistry *33*, 14281-14288.

Greenfield, N.J. (2004). Analysis of circular dichroism data. Methods in enzymology *383*, 282-317.

Gregersen, N. (2006). Protein misfolding disorders: pathogenesis and intervention. Journal of inherited metabolic disease *29*, 456-470.

Hakansson, K., Carlsson, M., Svensson, L.A., and Liljas, A. (1992). Structure of native and apo carbonic anhydrase II and structure of some of its anion-ligand complexes. Journal of molecular biology *227*, 1192-1204.

Hakansson, K., and Liljas, A. (1994). The structure of a complex between carbonic anhydrase II and a new inhibitor, trifluoromethane sulphonamide. FEBS letters *350*, 319-322.

Hammarstrom, P., Jiang, X., Hurshman, A.R., Powers, E.T., and Kelly, J.W. (2002). Sequence-dependent denaturation energetics: A major determinant in amyloid disease diversity. Proceedings of the National Academy of Sciences of the United States of America *99 Suppl 4*, 16427-16432.

Hammarstrom, P., Owenius, R., Martensson, L.G., Carlsson, U., and Lindgren, M. (2001a). High-resolution probing of local conformational changes in proteins by the use of multiple labeling: unfolding and self-assembly of human carbonic anhydrase II monitored by spin, fluorescent, and chemical reactivity probes. Biophysical journal *80*, 2867-2885.

Hammarstrom, P., Persson, M., and Carlsson, U. (2001b). Protein compactness measured by fluorescence resonance energy transfer. Human carbonic anhydrase ii is considerably expanded by the interaction of GroEL. The Journal of biological chemistry *276*, 21765-21775.

Hammarstrom, P., Persson, M., Freskgard, P.O., Martensson, L.G., Andersson, D., Jonsson, B.H., and Carlsson, U. (1999). Structural mapping of an aggregation nucleation site in a molten globule intermediate. The Journal of biological chemistry *274*, 32897-32903.

Harper, J.D., and Lansbury, P.T., Jr. (1997). Models of amyloid seeding in Alzheimer's disease and scrapie: mechanistic truths and physiological consequences of the time-dependent solubility of amyloid proteins. Annual review of biochemistry *66*, 385-407.

Hawe, A., Sutter, M., and Jiskoot, W. (2008). Extrinsic fluorescent dyes as tools for protein characterization. Pharmaceutical research *25*, 1487-1499.

Hentunen, T.A., Harkonen, P.L., and Vaananen, H.K. (2000). Carbonic anhydrases in calcified tissues. Exs, 491-497.

Hornemann, S., Schorn, C., and Wuthrich, K. (2004). NMR structure of the bovine prion protein isolated from healthy calf brains. EMBO reports *5*, 1159-1164.

Hornshaw, M.P., McDermott, J.R., Candy, J.M., and Lakey, J.H. (1995). Copper binding to the N-terminal tandem repeat region of mammalian and avian prion protein: structural studies using synthetic peptides. Biochemical and biophysical research communications *214*, 993-999.

Horovitz, A., Serrano, L., Avron, B., Bycroft, M., and Fersht, A.R. (1990). Strength and co-operativity of contributions of surface salt bridges to protein stability. Journal of molecular biology *216*, 1031-1044.

Hu, P.Y., Ernst, A.R., Sly, W.S., Venta, P.J., Skaggs, L.A., and Tashian, R.E. (1994). Carbonic anhydrase II deficiency: single-base deletion in exon 7 is the predominant mutation in Caribbean Hispanic patients. American journal of human genetics *54*, 602-608.

Hu, P.Y., Lim, E.J., Ciccolella, J., Strisciuglio, P., and Sly, W.S. (1997). Seven novel mutations in carbonic anhydrase II deficiency syndrome identified by SSCP and direct sequencing analysis. Human mutation *9*, 383-387.

Hu, P.Y., Roth, D.E., Skaggs, L.A., Venta, P.J., Tashian, R.E., Guibaud, P., and Sly, W.S. (1992). A splice junction mutation in intron 2 of the carbonic anhydrase II gene of osteopetrosis patients from Arabic countries. Human mutation *1*, 288-292.

Jimenez, J.L., Guijarro, J.I., Orlova, E., Zurdo, J., Dobson, C.M., Sunde, M., and Saibil, H.R. (1999). Cryo-electron microscopy structure of an SH3 amyloid fibril and model of the molecular packing. The EMBO journal *18*, 815-821.

Jimenez, J.L., Nettleton, E.J., Bouchard, M., Robinson, C.V., Dobson, C.M., and Saibil, H.R. (2002). The protofilament structure of insulin amyloid fibrils. Proceedings of the National Academy of Sciences of the United States of America *99*, 9196-9201.

Johnson, R.T. (2005). Prion diseases. Lancet neurology *4*, 635-642.

Johnson, R.T., and Gibbs, C.J., Jr. (1998). Creutzfeldt-Jakob disease and related transmissible spongiform encephalopathies. The New England journal of medicine *339*, 1994-2004.

Kelenyi, G. (1967). On the histochemistry of azo group-free thiazole dyes. J Histochem Cytochem *15*, 172-180.

Kelly, J.W. (2002). Towards an understanding of amyloidogenesis. Nature structural biology *9*, 323-325.

Kelly, S.M., Jess, T.J., and Price, N.C. (2005). How to study proteins by circular dichroism. Biochimica et biophysica acta *1751*, 119-139.

Kovacs, G.G., and Budka, H. (2008). Prion diseases: from protein to cell pathology. The American journal of pathology *172*, 555-565.

Kovacs, G.G., Puopolo, M., Ladogana, A., Pocchiari, M., Budka, H., van Duijn, C., Collins, S.J., Boyd, A., Giulivi, A., Coulthart, M., *et al.* (2005). Genetic prion disease: the EUROCJD experience. Human genetics *118*, 166-174.

Ladogana, A., Puopolo, M., Croes, E.A., Budka, H., Jarius, C., Collins, S., Klug, G.M., Sutcliffe, T., Giulivi, A., Alperovitch, A., *et al.* (2005). Mortality from Creutzfeldt-Jakob disease and related disorders in Europe, Australia, and Canada. Neurology *64*, 1586-1591.

Lakowicz, J.R. (2006). Principles of Fluoroscence Spectroscopy (New York, Springer science + Buisness media).

Lambert, M.P., Barlow, A.K., Chromy, B.A., Edwards, C., Freed, R., Liosatos, M., Morgan, T.E., Rozovsky, I., Trommer, B., Viola, K.L., *et al.* (1998). Diffusible, nonfibrillar ligands derived from Abeta1-42 are potent central nervous system neurotoxins. Proceedings of the National Academy of Sciences of the United States of America *95*, 6448-6453.

Le Pichon, C.E., Valley, M.T., Polymenidou, M., Chesler, A.T., Sagdullaev, B.T., Aguzzi, A., and Firestein, S. (2009). Olfactory behavior and physiology are disrupted in prion protein knockout mice. Nature neuroscience *12*, 60-69.

Lehtonen, J., Shen, B., Vihinen, M., Casini, A., Scozzafava, A., Supuran, C.T., Parkkila, A.K., Saarnio, J., Kivela, A.J., Waheed, A., *et al.* (2004). Characterization of CA XIII, a novel member of the carbonic anhydrase isozyme family. The Journal of biological chemistry *279*, 2719-2727.

LeVine, H., 3rd (1999). Quantification of beta-sheet amyloid fibril structures with thioflavin T. Methods in enzymology *309*, 274-284.

Levinthal, C. (1969). How to Fold Graciously. Paper presented at: Mossbauer Spectroscopy in Biological Systems (Monticello, Illinois, University of Illinois Press).

Linden, R., Martins, V.R., Prado, M.A., Cammarota, M., Izquierdo, I., and Brentani, R.R. (2008). Physiology of the prion protein. Physiological reviews *88*, 673-728.

Lindskog, S. (1997). Structure and mechanism of carbonic anhydrase. Pharmacology & therapeutics *74*, 1-20.

Linsell, L., Cousens, S.N., Smith, P.G., Knight, R.S., Zeidler, M., Stewart, G., de Silva, R., Esmonde, T.F., Ward, H.J., and Will, R.G. (2004). A case-control study of sporadic Creutzfeldt-Jakob disease in the United Kingdom: analysis of clustering. Neurology *63*, 2077-2083.

Luisi, D.L., Snow, C.D., Lin, J.J., Hendsch, Z.S., Tidor, B., and Raleigh, D.P. (2003). Surface salt bridges, double-mutant cycles, and protein stability: an experimental and computational analysis of the interaction of the Asp 23 side chain with the N-terminus of the N-terminal domain of the ribosomal protein l9. Biochemistry *42*, 7050-7060.

Makhatadze, G.I., Loladze, V.V., Ermolenko, D.N., Chen, X., and Thomas, S.T. (2003). Contribution of surface salt bridges to protein stability: guidelines for protein engineering. Journal of molecular biology *327*, 1135-1148.

Martensson, L.G., Jonsson, B.H., Andersson, M., Kihlgren, A., Bergenhem, N., and Carlsson, U. (1992). Role of an evolutionarily invariant serine for the stability of human carbonic anhydrase II. Biochimica et biophysica acta *1118*, 179-186.

Martensson, L.G., Jonsson, B.H., Freskgard, P.O., Kihlgren, A., Svensson, M., and Carlsson, U. (1993). Characterization of folding intermediates of human carbonic anhydrase II: probing substructure by chemical labeling of SH groups introduced by site-directed mutagenesis. Biochemistry *32*, 224-231.

Max, d.t. (2006). The family that could not sleep (New York, Random House).

Naiki, H., Higuchi, K., Hosokawa, M., and Takeda, T. (1989). Fluorometric determination of amyloid fibrils in vitro using the fluorescent dye, thioflavin T1. Analytical biochemistry *177*, 244-249.

Nielsen, L., Khurana, R., Coats, A., Frokjaer, S., Brange, J., Vyas, S., Uversky, V.N., and Fink, A.L. (2001). Effect of environmental factors on the kinetics of insulin fibril formation: elucidation of the molecular mechanism. Biochemistry *40*, 6036-6046.

Nieto, A., Goldfarb, L.G., Brown, P., McCombie, W.R., Trapp, S., Asher, D.M., and Gajdusek, D.C. (1991). Codon 178 mutation in ethnically diverse Creutzfeldt-Jakob disease families. Lancet *337*, 622-623.

Pepys, M.B. (2006). Amyloidosis. Annual review of medicine *57*, 223-241.

Perera, W.S., and Hooper, N.M. (2001). Ablation of the metal ion-induced endocytosis of the prion protein by disease-associated mutation of the octarepeat region. Curr Biol *11*, 519-523.

Perriman, A.W., Henderson, M.J., Holt, S.A., and White, J.W. (2007). Effect of the air-water interface on the stability of beta-lactoglobulin. The journal of physical chemistry *111*, 13527-13537.

Persson, M., Hammarstrom, P., Lindgren, M., Jonsson, B.H., Svensson, M., and Carlsson, U. (1999). EPR mapping of interactions between spin-labeled variants of human carbonic anhydrase II and GroEL: evidence for increased flexibility of the hydrophobic core by the interaction. Biochemistry *38*, 432-441.

Prusiner, S.B. (1982). Novel proteinaceous infectious particles cause scrapie. Science (New York, NY *216*, 136-144.

Prusiner, S.B. (1994). Molecular biology and genetics of prion diseases. Philosophical transactions of the Royal Society of London *343*, 447-463.

Prusiner, S.B., McKinley, M.P., Bowman, K.A., Bolton, D.C., Bendheim, P.E., Groth, D.F., and Glenner, G.G. (1983). Scrapie prions aggregate to form amyloid-like birefringent rods. Cell *35*, 349-358.

Rettig, W. (1986). Charge Separation in Excited States of Decoupled Systems - TICT Compounds and Implications Regarding the Development of New Laser Dyes and the Primary Process of Vision and Photosynthesis Angewandte Chemie International Edition *25*, 971-988.

Rickli, E.E., Ghazanfar, S.A., Gibbons, B.H., and Edsall, J.T. (1964). Carbonic Anhydrases from Human Erythrocytes. Preparation and Properties of Two Enzymes. The Journal of biological chemistry *239*, 1065-1078.

Ridderstrale, Y., and Hanson, M. (1985). Histochemical study of the distribution of carbonic anhydrase in the cat brain. Acta physiologica Scandinavica *124*, 557-564.

Roth, D.E., Venta, P.J., Tashian, R.E., and Sly, W.S. (1992). Molecular basis of human carbonic anhydrase II deficiency. Proceedings of the National Academy of Sciences of the United States of America *89*, 1804-1808.

Ruska, E. (1986). The Development of the Electron Microscope and of Electron Microscopy. In Nobel Lectures, Physics 1981-1990,, T. Frängsmyr, ed. (Singapore, World Scientific Publishing Co).

Sali, A., Shakhnovich, E., and Karplus, M. (1994). How does a protein fold? Nature *369*, 248-251.

Santoro, M.M., and Bolen, D.W. (1988). Unfolding free energy changes determined by the linear extrapolation method. 1. Unfolding of phenylmethanesulfonyl alpha-chymotrypsin using different denaturants. Biochemistry *27*, 8063-8068.

Serio, T.R., Cashikar, A.G., Kowal, A.S., Sawicki, G.J., Moslehi, J.J., Serpell, L., Arnsdorf, M.F., and Lindquist, S.L. (2000). Nucleated conformational conversion and the replication of conformational information by a prion determinant. Science (New York, NY *289*, 1317-1321.

Serpell, L.C., Sunde, M., Benson, M.D., Tennent, G.A., Pepys, M.B., and Fraser, P.E. (2000). The protofilament substructure of amyloid fibrils. Journal of molecular biology *300*, 1033-1039.

Shah, G.N., Bonapace, G., Hu, P.Y., Strisciuglio, P., and Sly, W.S. (2004). Carbonic anhydrase II deficiency syndrome (osteopetrosis with renal tubular acidosis and brain calcification): novel mutations in CA2 identified by direct sequencing expand the opportunity for genotype-phenotype correlation. Human mutation *24*, 272.

Shah, G.N., Hewett-Emmett, D., Grubb, J.H., Migas, M.C., Fleming, R.E., Waheed, A., and Sly, W.S. (2000). Mitochondrial carbonic anhydrase CA VB: differences in tissue distribution and pattern of evolution from those of CA VA suggest distinct physiological roles. Proceedings of the National Academy of Sciences of the United States of America *97*, 1677-1682.

Shortle, D. (1996). The denatured state (the other half of the folding equation) and its role in protein stability. Faseb J *10*, 27-34.

Simoneau, S., Rezaei, H., Sales, N., Kaiser-Schulz, G., Lefebvre-Roque, M., Vidal, C., Fournier, J.G., Comte, J., Wopfner, F., Grosclaude, J., *et al.* (2007). In vitro and in vivo neurotoxicity of prion protein oligomers. PLoS pathogens *3*, e125.

Sluzky, V., Tamada, J.A., Klibanov, A.M., and Langer, R. (1991). Kinetics of insulin aggregation in aqueous solutions upon agitation in the presence of hydrophobic surfaces. Proceedings of the National Academy of Sciences of the United States of America *88*, 9377-9381.

Sly, W.S., Hewett-Emmett, D., Whyte, M.P., Yu, Y.S., and Tashian, R.E. (1983). Carbonic anhydrase II deficiency identified as the primary defect in the autosomal recessive syndrome of osteopetrosis with renal tubular acidosis and cerebral calcification. Proceedings of the National Academy of Sciences of the United States of America *80*, 2752-2756.

Sly, W.S., and Hu, P.Y. (1995). Human carbonic anhydrases and carbonic anhydrase deficiencies. Annual review of biochemistry *64*, 375-401.

Sly, W.S., Whyte, M.P., Sundaram, V., Tashian, R.E., Hewett-Emmett, D., Guibaud, P., Vainsel, M., Baluarte, H.J., Gruskin, A., Al-Mosawi, M., *et al.* (1985). Carbonic anhydrase II deficiency in 12 families with the autosomal recessive syndrome of osteopetrosis with renal tubular acidosis and cerebral calcification. The New England journal of medicine *313*, 139-145.

Smith, L.J., Fiebig, K.M., Schwalbe, H., and Dobson, C.M. (1996). The concept of a random coil. Residual structure in peptides and denatured proteins. Folding & design *1*, R95-106.

Soda, H., Yukizane, S., Yoshida, I., Aramaki, S., and Kato, H. (1995). Carbonic anhydrase II deficiency in a Japanese patient produced by a nonsense mutation (TAT-->TAG) at Tyr-40 in exon 2, (Y40X). Human mutation *5*, 348-350.

Soda, H., Yukizane, S., Yoshida, I., Koga, Y., Aramaki, S., and Kato, H. (1996). A point mutation in exon 3 (His 107-->Tyr) in two unrelated Japanese patients with carbonic anhydrase II deficiency with central nervous system involvement. Human genetics *97*, 435-437.

Sorgjerd, K., Klingstedt, T., Lindgren, M., Kagedal, K., and Hammarstrom, P. (2008). Prefibrillar transthyretin oligomers and cold stored native tetrameric transthyretin are cytotoxic in cell culture. Biochemical and biophysical research communications *377*, 1072-1078.

Sousa, M.M., Yan, S.D., Stern, D., and Saraiva, M.J. (2000). Interaction of the receptor for advanced glycation end products (RAGE) with transthyretin triggers nuclear transcription factor kB (NF-kB) activation. Laboratory investigation; a journal of technical methods and pathology *80*, 1101-1110.

Spencer, M.D., Knight, R.S., and Will, R.G. (2002). First hundred cases of variant Creutzfeldt-Jakob disease: retrospective case note review of early psychiatric and neurological features. BMJ (Clinical research ed *324*, 1479-1482.

Stefani, M., and Dobson, C.M. (2003). Protein aggregation and aggregate toxicity: new insights into protein folding, misfolding diseases and biological evolution. Journal of molecular medicine (Berlin, Germany) *81*, 678-699.

Steiner, H., Jonsson, B.H., and Lindskog, S. (1975). The catalytic mechanism of carbonic anhydrase. Hydrogen-isotope effects on the kinetic parameters of the human C isoenzyme. European journal of biochemistry / FEBS *59*, 253-259.

Stockel, J., Safar, J., Wallace, A.C., Cohen, F.E., and Prusiner, S.B. (1998). Prion protein selectively binds copper(II) ions. Biochemistry *37*, 7185-7193.

Stohr, J., Weinmann, N., Wille, H., Kaimann, T., Nagel-Steger, L., Birkmann, E., Panza, G., Prusiner, S.B., Eigen, M., and Riesner, D. (2008). Mechanisms of prion protein assembly into amyloid. Proceedings of the National Academy of Sciences of the United States of America *105*, 2409-2414.

Sun, M.K., and Alkon, D.L. (2002). Carbonic anhydrase gating of attention: memory therapy and enhancement. Trends in pharmacological sciences *23*, 83-89.

Sundaram, V., Rumbolo, P., Grubb, J., Strisciuglio, P., and Sly, W.S. (1986). Carbonic anhydrase II deficiency: diagnosis and carrier detection using differential enzyme inhibition and inactivation. American journal of human genetics *38*, 125-136.

Sundquist, K., Lakkakorpi, P., Wallmark, B., and Vaananen, K. (1990). Inhibition of osteoclast proton transport by bafilomycin A1 abolishes bone resorption. Biochemical and biophysical research communications *168*, 309-313.

Supuran, C.T. (2008). Carbonic anhydrases: novel therapeutic applications for inhibitors and activators. Nature reviews *7*, 168-181.

Swenson, E.R. (2000). Respiratory and renal roles of carbonic anhydrase in gas exchange and acid-base regulation. Exs, 281-341.

Svensson, M., Jonasson, P., Freskgard, P.O., Jonsson, B.H., Lindgren, M., Martensson, L.G., Gentile, M., Boren, K., and Carlsson, U. (1995). Mapping the folding intermediate of human carbonic anhydrase II. Probing substructure by chemical reactivity and spin and fluorescence labeling of engineered cysteine residues. Biochemistry *34*, 8606-8620.

Tan, S.Y., and Pepys, M.B. (1994). Amyloidosis. Histopathology *25*, 403-414.

Temperini, C., Scozzafava, A., Puccetti, L., and Supuran, C.T. (2005). Carbonic anhydrase activators: X-ray crystal structure of the adduct of human isozyme II with L-histidine as a platform for the design of stronger activators. Bioorganic & medicinal chemistry letters *15*, 5136-5141.

Temperini, C., Scozzafava, A., Vullo, D., and Supuran, C.T. (2006a). Carbonic anhydrase activators. Activation of isoforms I, II, IV, VA, VII, and XIV with L- and D-phenylalanine and crystallographic analysis of their adducts with isozyme II:

stereospecific recognition within the active site of an enzyme and its consequences for the drug design. Journal of medicinal chemistry *49*, 3019-3027.

Temperini, C., Scozzafava, A., Vullo, D., and Supuran, C.T. (2006b). Carbonic anhydrase activators. Activation of isozymes I, II, IV, VA, VII, and XIV with l- and d-histidine and crystallographic analysis of their adducts with isoform II: engineering proton-transfer processes within the active site of an enzyme. Chemistry (Weinheim an der Bergstrasse, Germany) *12*, 7057-7066.

Thomas, P.J., Qu, B.H., and Pedersen, P.L. (1995). Defective protein folding as a basis of human disease. Trends in biochemical sciences *20*, 456-459.

Tissot, A.C., Vuilleumier, S., and Fersht, A.R. (1996). Importance of two buried salt bridges in the stability and folding pathway of barnase. Biochemistry *35*, 6786-6794.

Tu, C.K., Silverman, D.N., Forsman, C., Jonsson, B.H., and Lindskog, S. (1989). Role of histidine 64 in the catalytic mechanism of human carbonic anhydrase II studied with a site-specific mutant. Biochemistry *28*, 7913-7918.

Wadsworth, J.D., and Collinge, J. (2007). Update on human prion disease. Biochimica et biophysica acta *1772*, 598-609.

Wadsworth, J.D., Hill, A.F., Beck, J.A., and Collinge, J. (2003). Molecular and clinical classification of human prion disease. British medical bulletin *66*, 241-254.

Wang, L., Maji, S.K., Sawaya, M.R., Eisenberg, D., and Riek, R. (2008). Bacterial inclusion bodies contain amyloid-like structure. PLoS biology *6*, e195.

Vassar, P.S., and Culling, C.F. (1959). Fluorescent stains, with special reference to amyloid and connective tissues. Archives of pathology *68*, 487-498.

Weber, A., Casini, A., Heine, A., Kuhn, D., Supuran, C.T., Scozzafava, A., and Klebe, G. (2004). Unexpected nanomolar inhibition of carbonic anhydrase by COX-2-selective celecoxib: new pharmacological opportunities due to related binding site recognition. Journal of medicinal chemistry *47*, 550-557.

Venta, P.J., Welty, R.J., Johnson, T.M., Sly, W.S., and Tashian, R.E. (1991). Carbonic anhydrase II deficiency syndrome in a Belgian family is caused by a point mutation at an invariant histidine residue (107 His----Tyr): complete structure of the normal human CA II gene. American journal of human genetics *49*, 1082-1090.

Wetzel, R. (2002). Ideas of order for amyloid fibril structure. Structure *10*, 1031-1036.

Vidgren, J., Liljas, A., and Walker, N.P. (1990). Refined structure of the acetazolamide complex of human carbonic anhydrase II at 1.9 A. International journal of biological macromolecules *12*, 342-344.

Will, R.G., Ironside, J.W., Zeidler, M., Cousens, S.N., Estibeiro, K., Alperovitch, A., Poser, S., Pocchiari, M., Hofman, A., and Smith, P.G. (1996). A new variant of Creutzfeldt-Jakob disease in the UK. Lancet *347*, 921-925.

Volles, M.J., and Lansbury, P.T., Jr. (2003). Zeroing in on the pathogenic form of alpha-synuclein and its mechanism of neurotoxicity in Parkinson's disease. Biochemistry *42*, 7871-7878.

Wolynes, P.G., Onuchic, J.N., and Thirumalai, D. (1995). Navigating the folding routes. Science (New York, NY *267*, 1619-1620.

Wroe, S.J., Pal, S., Siddique, D., Hyare, H., Macfarlane, R., Joiner, S., Linehan, J.M., Brandner, S., Wadsworth, J.D., Hewitt, P., *et al.* (2006). Clinical presentation and pre-mortem diagnosis of variant Creutzfeldt-Jakob disease associated with blood transfusion: a case report. Lancet *368*, 2061-2067.

Zahn, R., Liu, A., Luhrs, T., Riek, R., von Schroetter, C., Lopez Garcia, F., Billeter, M., Calzolai, L., Wider, G., and Wuthrich, K. (2000). NMR solution structure of the human prion protein. Proceedings of the National Academy of Sciences of the United States of America *97*, 145-150.